International
Progress Report

IPR-99-19

Äspö Hard Rock Laboratory

Redox experiment in detailed scale (REX):

Laboratory work to excamine microbial effects on redox and quantification of the effects of microbiological perturbations on the geological disposal of HLW (TRU)

H Yoshida, K Hama
Japan Nuclear Cycle Development Institute, Japan

J M West, K Bateman, A E Milodowski, S J Baker,
P Coombs, V L Hards, B Spiro, P D Wetton
British Geological Survey, UK

July 1999

Svensk Kärnbränslehantering AB
Swedish Nuclear Fuel
and Waste Management Co
Box 5864
SE-102 40 Stockholm Sweden
Tel 08-459 84 00
+46 8 459 84 00
Fax 08-661 57 19
+46 8 661 57 19

Äspö Hard Rock Laboratory

Report no.
IPR-99-19
Author
H Yoshida et al
Checked by
Peter Wikberg
Approved
Olle Olsson

No.
F57K
Date
July 1999
Date
1999-09-20
Date
1999-09-22

Äspö Hard Rock Laboratory

Redox experiment in detailed scale (REX):

Laboratory work to examine microbial effects on redox and quantification of the effects of microbiological perturbations on the geological disposal of HLW (TRU)

H Yoshida, K Hama

Japan Nuclear Cycle Development Institute, Japan

J M West, K Bateman, A E Milodowski, S J Baker, P Coombs, V L Hards, B Spiro, P D Wetton

British Geological Survey, UK

July 1999

Keywords: Microbial geochemistry, Subsurface biology, Microbial redox activity

PREFACE

In April 1997 the Japan Nuclear Cycle Development Institute (JNC) commissioned a Three-Task project from the British Geological Survey (BGS). Task 1 was a continuation of work started in 1996 to examine microbial effects on redox and to quantify the effects of microbiological perturbations on the geological disposal of HLW (TRU). Task 2 was commissioned to provide information on the Tsukiyoshi Fault for use in ongoing work at the Tono Geoscience Centre. Task 3 was to draft a Technical programme for a geochemical study of the Tono site.

This report details the results of Task 1, undertaken in 1998/99.

CONTENTS

1. INTRODUCTION

The Japan Nuclear Cycle Development Institute (JNC) is currently undertaking a joint research programme with the Swedish Nuclear Fuel and Waste Management Company (SKB). The purpose of this research is to investigate the capability of the near-repository host rock to consume dissolved oxygen in groundwater remaining in the backfill and near-field rock following the operational phase of a radioactive waste repository. These investigations will be carried out *in situ* in a single, well defined hydraulically-conductive fracture within SKB's underground research facility at the Äspö Hard Rock Laboratory (Figure 1), Äspö Island, south eastern Sweden.

The British Geological Survey (BGS) was contracted by JNC to participate in this study using laboratory studies to evaluate the microbiological effects influencing redox, particularly in a situation where oxygen ingress occurs. The results from Year 1 and Year 2 are given in West *et al* (1997) and West (1998).

2. BACKGROUND

During the construction and operation of a deep repository for high level waste (HLW), the subsurface environment will be open to oxidising surface conditions and surface water inflow. The Äspö Redox investigations in Block scale, reported in Banwart (1995), investigated the possibility of oxygen ingress into vertical fracture zones which may occur during repository construction due to increased surface inflow.

In this study a hydraulically vertical fracture zone, which had been intersected at 70m depth during tunnel construction, had shown that oxidising surface waters rapidly mixed with the original saline waters. However, intensive anaerobic respiration by microorganisms resulted from the increased recharge. There appeared to be an inflow of reducing capacity in the form of 'young' surface organic carbon rather than oxygen at 70m, presumably because oxygen and other oxidants had been scavenged by microbes at shallower depths. Thus, after an initial oxic period, the fracture zone remained persistently anoxic. It was proposed that the microbial processes involved included anaerobic respiration coupled to reduction of iron hydroxide, methanogenesis, precipitation of calcite and secondary ferrous minerals. The operation of these processes is considered to have significant implications for radionuclide solubility and sorption, stability and mobility of colloids and speciation. The Redox Experiment in detailed Scale (REX) study was set up as a result of this work to further study redox experiments but in a more controlled manner.

3. THE REX PROJECT AND COMPLEMENTARY LABORATORY STUDIES AT BGS

The objective of the REX Project is to investigate oxygen consumption in a simulated repository by creating a controlled oxidising perturbation to the deep rock environment at Äspö. The specific objectives of the programme are:

- Assess the capacity of the host rock to buffer against oxidising disturbance.
- Determine the kinetics (half life) of oxygen consumption.
- Apply quantitative descriptions of these processes, which can be used in performance assessment of the repository redox stability for the post-closure phase.
- Demonstrate the capacity of oxidised rock surfaces to retard uranium migration after oxidation of the rock.

The work carried out and described in this report is a complementary laboratory study to the REX programme. It examines the interaction of microbes with mineralogical surfaces involved with groundwater flow. As has been recognised, fracture flow will dominate groundwater movement at Äspö. The mineralogical nature of the fracture surfaces and subsequent changes to those surfaces will be important with regard to radionuclide sorption and retardation, and also with respect to buffering groundwater redox through rock-water interaction. The mineralogy of the surfaces will also be important with respect to microbial interaction in terms of redox reactions mediated by microbial activity, and in providing substrates for microbes. Thus, the study required a multi-disciplinary approach involving collection of fracture material and construction of experiments designed to simulate bacterial interactions in the Äspö fracture groundwater system.

The experiments were started in Year 1 (1996) using batch systems and a complete interpretation of the results was given in West (1998). Results showed the microbes potentially have complicated effects on the geochemistry of the system. At the end of Year 2, a series of flow through columns were set up under anaerobic conditions. However, problems were encountered with blocking of the columns shortly after the experiments started. Consequently, a series of continuously flowing cells were set up in Year 3 which ran under both anaerobic and aerobic conditions. This report describes the results of both the column experiments and the flowing cells.

4. GEOLOGICAL BACKGROUND

4.1 Bedrock geology of the Äspö site

For a detailed account of the geology, structure and fracturing characteristics of the Äspö site, the reader is referred to West *et al* (1997) and West (1998) and references therein.

4.2 The REX Experimental Block

The location of the area designated for the REX Experimental Block is described in the SELECT Report (Winberg *et al.*, 1996). Two fully-cored low-angle/sub-horizontal boreholes, KA2858A and KA2862A, have been drilled at this site (Figure 2) in order to evaluate the geology, hydrogeology and fracture characteristics. These two boreholes have been the subject of the detailed fracture mineral logging reported in West *et al* (1997) and West (1998).

The geology of the block has been described by Winberg *et al.* (1996). It consists of Småland Granite west of L=2/850m and Äspö Diorite east of L=2/850m (refer to long-tunnel (upper level) measurements shown in Figure 2). The main structural elements in the REX Experimental Block area are shown in Figure 2. Two 20m wide zones of ductile fracturing cross the tunnel at L=2/760 and 2/830m (not shown in Figure 2). No groundwater discharge is seen where these two fracture zones intersect the Äspö tunnel. Two 0.5m wide NE-trending ductile fracture zones cross the tunnel at L=2/740 and 2/865 m. A thrust, trending NE and dipping 50%SE, intersects the tunnel at L=2/760. A second NE-trending thrust dips 25%SE and intersects the tunnel leg at the overlying tunnel, Z=250m, at L=1/830m.

The main hydrogeological features are shown, in simplified form, in Figure 2. To the northwest, the block is bounded by a large NE-trending ductile fracture zone (estimated transmissivity (Winberg *et al.*, 1996) = $4x10^{-7}$-$1x10^{-4}$ m^2s^{-1}) referred to as EW-1. This consists of two main branches associated with intense fracturing, mylonitisation and hydrothermal alteration. The eastern edge of the block is delineated by a NNW-trending fracture zone (NNW-4) which intersects the tunnel at L=2/930m. NNW-4 is considered to be highly conductive (Winberg *et al.*, 1996), with an estimated transmissivity of up to $1x10^{-4}$ m^2s^{-1}, where it intersects the higher levels of the Äspö tunnel. The south side of the block is hydrologically bounded by a NW-trending fault zone (NW-3) which intersects the tunnel at L=2/910m, and intersects Zone NNW-4 immediately south of the tunnel at L=2/930m.

The lithology of Borehole KA2858A is dominated by Äspö Diorite (62.3% of sequence), but sections of Småland Granite (12.1% of sequence) and fine-grained granite (25.6% of sequence) are encountered between 5-20m distance, and towards the end of the borehole between 43-60m distance (Winberg *et al.*, 1996). The borehole intersects a set of fractures with a trend of N20E. In this region the core is locally strongly foliated, chloritised and reddened. Core 'disking' occurs at L=12.6m, associated with bodies of fine grained granite, separating Småland Granite from Äspö Diorite. Groundwater flow was detected during drilling at 44.66m (0.3 l/m), and subsequent hydrogeological testing indicated that the bulk of groundwater flow in the borehole is attributable to a flow-zone between 40.0-40.7m. The borehole terminates at 59.70m.

Borehole KA2862A lies entirely within the Äspö Diorite, and also intersects zones of N20E-trending fractures (Winberg *et al.*, 1996). The core, in part, is strongly foliated, chloritised and reddened. During drilling, the borehole remained dry until a depth of 10.37m when groundwater inflow was intersected (0.15 l/m). From 11.20m the core is foliated and altered along N20E-trending epidote-chlorite-mineralised fractures. The end of the borehole intersects a zone of N60-70W-trending calcite- and chlorite-mineralised fractures (one at L=15.5m dips 85%SE; four parallel fractures between L=15.65-15.80 dip 85%NE). These fractures are considered to be the margins of the major fracture zone, NW-3. The water flow into the borehole increases to about 2.0 l/m from about 15m depth. The borehole terminates at 15.98m.

5. FIELD SAMPLING AND CHARACTERISATION OF STARTING MATERIALS FOR EXPERIMENTS

5.1 Field Sampling

A brief field visit was made to the Äspö Hard Rock Laboratory, Äspö Island, Figholm, Sweden during 16-17 September 1997 in order to collect further samples of groundwater and Äspö Diorite for use in the Year 2 Laboratory Experimental Programme. As in Year 1, the samples were all collected from the REX alcove in the underground laboratory. A full description of the sampling site is provided West (1998).

5.2 Groundwater sampling

Groundwater samples were taken from a gently inclined, sub-horizontal borehole - borehole KA2858A - which had previously been sampled for the Year 1 laboratory experiments (West *et al.*, 1997). This borehole has been completed with three packered intervals: Section 1 samples water entering the borehole between 6.02 and 38.77m; Section 2 samples the borehole between 39.77 and 40.77m; and Section 3 samples the borehole between 41.77 and 59.77m from the tunnel wall. Section 2 was sampled for use in the BGS experiments.

Two 20 litre samples were collected anaerobically using special stainless steel flasks. These were fitted with an inlet tube that reached to the base of the flask and an outlet tube at the top. Both the inlet and outlet had spring-loaded needle-valves that opened when the clip-fit connecting pressure hoses were fitted, and these sealed the vessel automatically once the hoses were removed. The vessels were rinsed three times with water from borehole KA2858A before sample collection and then flushed for 20 minutes with oxygen-free nitrogen before filling with the groundwater. Subsequently, the flasks were connected to the discharge line from Section 2 of the borehole and filled from the bottom-upwards, (displacing the nitrogen-top atmosphere as they were filled with water). The two vessels were connected in series during filling, and a bubble trap was fitted at the outlet to the second flask to prevent any back-diffusion of atmospheric oxygen during the sampling operation.

The borehole was opened and allowed to discharge three borehole-volumes of groundwater before any sampling started. This was done in order to flush out any 'stagnant' groundwater residing within the borehole. During this process, the flow was measured by timing the

collection of a measured volume of groundwater in a large measuring cylinder. The groundwater discharge from Section 2 of borehole KA2858A was estimated to be 0.22 litres/minute.

The groundwater was also sub-sampled for chemical analysis. Samples for analysis were collected immediately before filling, and immediately after filling, the large stainless steel sampling flasks. Eh (±0.1 mV), pH (±0.01 pH unit), temperature (±0.1°C) and conductivity were determined during sampling using portable meters (Orion Research Model SA250) fitted with specific ion electrodes. The Eh was measured with a standard Pt-Ag/AgCl electrode verified with Zobell's Solution (standard solution Eh = 200-250 mV). Eh readings were corrected for temperature (corrected Eh = uncorrected Eh + (244-T), where T is the temperature in degrees Celsius). The pH electrode was calibrated using standard pH4 and pH7 buffer solutions. The conductivity electrode was calibrated using a standard KCl solution.

Dissolved O_2 was determined in the field using a commercially available small portable colorimetric test kit (CHEMetrics). This contained pre-prepared vials of colorimetric reagent, sealed under vacuum, into which a fixed volume of groundwater was taken up when the tip of the vial was broken whilst immersed in the groundwater sample. The colour developed was assessed visually by comparison with a set of vials of standard concentrations for a range of dissolved oxygen contents from 1 to 12 ppm.

Bicarbonate was determined in the field by titration using a portable mechanical autotitrator kit. The water sample (25 ml) was titrated with standard sulphuric acid using Bromocresol Green indicator solution. Titrations were checked in the field against a 200 ppm bicarbonate standard solution that had been pre-prepared at BGS.

Water samples for subsequent chemical analysis at BGS were collected, filtered and preserved in the field. A 30 ml sample for major and trace cation analysis was collected directly into a plastic syringe. This was then filtered 'on-line' through a 0.45 μm pore diameter Acrodisc nylon filter, directly into Nalgene bottles. Samples were preserved by acidification to 1% with respect to AristaR nitric acid. Acid used in sample preservation was measured and dispensed using a hand-held autopipette. A 30 ml sample was similarly collected and filtered for ammonium analysis. However, this was preserved by acidification with 2 ml of AristaR sulphuric acid. A 30 ml sample for major and trace anions, total inorganic carbon (TIC) and total organic carbon (TOC)

was collected in a similar manner as for major and trace cations, except the water samples remained unacidified. Samples for determination of reduced Fe were taken and preserved by collecting and filtering 'on-line' through a 0.45 μm pore diameter Acrodisc nylon filter directly into Sterylin plastic tubes to which 1 ml of 1% 2,2-bipyridyl solution (HCl acidified) had been added. The volume was made up to 10 ml total with the sample. The 2,2-bipyridyl forms a stable red-coloured complex with ferrous iron in solution. A 30 ml sample of unfiltered water was collected for subsequent analysis of reduced sulphur. This was preserved by the addition of two pellets of sodium hydroxide. Blank samples for each of these preservations, using double-distilled water, were also prepared on-site.

5.3 Rock sampling

A large ($\approx$ 15-20 kg) block of diorite was collected from the tunnel wall within the REX alcove in the Äspö Hard Rock Laboratory, from the same location as that previously sampled during Year 1 (Milodowski *et al.*, 1996; West *et al.*, 1997). The sample was taken from the right-hand wall (down-tunnel side) of the REX alcove, located at the level of, and approximately 3m from, the position of borehole KA2862A (refer to Milodowski *et al.*, 1996 for further locational information).

Both rock and water samples were couriered to BGS by SKB upon completion of the sampling visit. On receipt of the samples by BGS in the United Kingdom, the large-volume water samples (in the stainless steel flasks) were placed in cold storage at 5°C until required for use in the Year 2 laboratory experiments.

5.4 Preparation of diorite experimental starting material

The experimental work requires crushed material within a limited grain-size range of 125-250 μm (hereafter referred to as the 'sand fraction'). The sample itself was composed of a solid block, $\approx$ 50 cm in length, bounded by fracture planes. It was first scrubbed to remove surface contamination, then jaw crushed. A representative sub-sample of the jaw crushed material was retained for analysis while the remainder was further prepared by wet-sieving to pass a 250 μm sieve. The <250 μm material was then sieved on 125 μm. Sub-samples of the retained jaw crushed material, the sand fraction and fines (<125 μm) were then tema-milled for subsequent analytical work to assess any fractionation that had resulted from the particle-size splitting of the sample.

5.5 Analytical methodology

5.5.1 Groundwater analyses

The samples of groundwater collected from the Äspö Hard Rock Laboratory were chemically analysed at the BGS. HCO_3^- was determined by automatic titration with 0.01 M sulphuric acid. Ca, Mg, Na, K, Total P, Total S, Si, Ba, Sr, Mn, Total Fe, Al, Co, Ni, Cu, Zn, Cr, Mo, Cd, Pb, V, Li and B were analysed by inductively-coupled plasma - atomic emission spectrometry (ICP-AES). Cl, Br, SO_4^{2-}, NO_3^-, NO_2^- and HPO_4^{2-} were determined by ion chromatography. F was analysed by ion-selective electrode. The analysis of TIC and TOC was performed using an automated total carbon analyser with a non-dispersive infrared detector. Reduced S was determined by hydride generation ICP-AES. Flow-injection analysis coupled with colorimetric analysis was used for the determination of NH_4. Reduced Fe was determined by ultraviolet/visible spectrophotometry. The field measurement of pH, Eh, temperature, conductivity, HCO_3^- and dissolved O_2 have been described above.

5.5.2 Petrographic analysis of Äspö Diorite sample

Two standard thin sections were prepared from the Äspö Diorite starting material (MPG sample D337), one from the outer edge (section P1) and one from the centre (section P2) to give a measure of heterogeneity in the material. Optical petrographic observations were made using a high-quality Zeiss optical petrographic microscope. Photomicrographs were taken using a Zeiss Ultraphot photomicroscope fitted with a Zeiss M35 camera on 200 ASA Kodak Gold film.

5.5.3 X-ray diffraction analysis of Äspö Diorite sample

X-ray diffraction (XRD) analysis was undertaken on both the bulk diorite sample (MPG sample D337), the sand fraction prepared for use in further BGS laboratory experiments and the removed fines (which were to be discarded). The aim of this was to assess any mineralogical fractionation that may have occurred in the preparation and cleaning-up of the sand-grade fraction material intended for use in the BGS column experiments. A representative sub-sample ($\approx$ 3g), of each of the tema-milled materials was micronised under acetone for five minutes. The resulting powders were then dried in an oven at 55°C and backloaded into standard aluminium sample holders. XRD analysis was carried out as described in West (1998).

5.5.4 Geochemistry of Äspö Diorite sample

Major and trace elements were determined by X-ray fluorescence analysis (XRF). XRF was undertaken using two sequential, fully automated, wavelength dispersive XRF spectrometers (Philips PW2400 and Philips PW1480/10 XRF spectrometers) fitted with a 60 kV generator and 3 kW rhodium ('Super Sharp') end-window X-ray tube, and a 100 kW and 3 kW tungsten side-window X-ray tube respectively.

Major element analysis of the bulk-rock and sand fraction was carried out to determine SiO_2, TiO_2, Al_2O_3, Fe_2O_3 (total), MnO, MgO, CaO, Na_2O, K_2O, P_2O_5, BaO and SrO contents. Samples were tema milled and finely powdered, then loss on ignition (LOI) was determined by heating samples to 1050°C. Analyte angles were calibrated from international and in-house standard reference materials. All standards and unknowns were prepared as fused glass discs using di-lithium tetraborate flux at approximately 1200°C. Drift correction was catered for by an external ratio monitor, and background corrections applied where necessary. It should be noted that Fe_2O_3 (total) determined represents the total Fe content of the samples.

Trace elements were determined by XRF using pressed powder pellets. Pellets were prepared by grinding representative splits of the powdered samples with Elvacite 2013 binder (Dupont n-butyl methacrylate copolymer) in an agate planetary ball mill, followed by pressing at 25 tons load into 40 mm diameter pellets.

5.6 Results and discussion

5.6.1 Groundwater analyses

Groundwater chemical analyses are presented in Table 1. Although the data are not discussed in detail here, since this is beyond the remit of the study, a number of features were noted. These are briefly described below.

It is apparent from the data that the composition of the groundwater changed during collection of the large-volume (40 litres) samples. The concentration of most species (with the exception of Field HCO_3^-, F, TIC, reduced S, Si, Al, and B, which show a decrease in concentration) increased from the start of sampling to the completion of sampling. The changes are significantly large for Eh, pH, Ca, Na, K, Cl, SO_4, Br, Total S, reduced S, Ba and Sr. Dissolved

O_2, Total P, NH_4^-, Co, Ni, Cu, Zn, Cr, Cd, Pb and V were all below analytical detection limit. These changes during groundwater production most probably reflect differences in chemistry between the groundwater in the 'disturbed zone' in the host rock immediately adjacent to the borehole wall - which would have been sampled initially, and more distant 'background' water which would have been sampled in the later stages of production. Because of this variation, it is recommended that an average of the two analyses be used in the setting up of the laboratory experiments and in subsequent use of the large volume water samples.

There are also significant differences between the field and subsequent laboratory pH analyses. Field pH is 0.99 to 1.3 pH units higher than measurements performed subsequently in the laboratory at BGS. It was noted during sampling that the groundwater effervesced strongly as it discharged from the borehole (see also previous sampling for Year 1, in West *et al.*, 1997). Thus, it is likely that outgassing continued to occur in the subsamples collected for laboratory analysis of anion species. Outgassing of CO_2 will strongly influence the pH and this may be responsible for the observed discrepancy between the field and laboratory analyses.

5.6.2 Petrographic analysis of Äspö Diorite sample

(a) Hand specimen description

The Äspö Diorite sample collected from the walls of the REX alcove in September 1997 (sample D337) is coarse-grained igneous rock. It is composed of approximately 50 % rounded, pink alkali feldspar (up to 4 mm) and approximately 10 % colourless/white quartz surrounded by a finer-grained Mafia mineral assemblage dominated by biotite mica.

(b) Thin section petrography

Petrographic analysis showed the diorite starting material (MPG sample D337) is a hydrothermally altered, partially recrystallised diorite. Two thin sections were cut, one from the edge of the sample and a second from the centre; comparison of the two confirmed the sample to be relatively homogeneous.

Examination of the thin sections, using a petrographic microscope, showed that the diorite sample is composed of major primary alkali feldspars, quartz and equant opaques, accompanied by secondary interstitial phases including: abundant green/brown biotite, epidote, carbonate, and accessory muscovite and sphene - possibly replacing ilmenite as the Ti-host. The feldspar

crystals reach 2.5 mm in length, are heavily sericitised, are generally untwinned, and include a few string perthites exsolution lamellae. The quartz has been partially recrystallised and shows lobate, sutured margins, strain extinction and the development of subgrains. The biotite forms irregular, randomly oriented flakes and is often intergrown with anhedral epidote.

5.6.3 XRD analysis of Äspö Diorite

XRD analysis of the bulk crushed diorite sample (whole rock, pre- removal of fines) was found to comprise major quartz and albite along with minor amounts of orthoclase, mica and chlorite, and traces of hematite, calcite and possibly cristobalite. Changes in mineralogy between the whole rock (pre-removal of fines) and the sand (with fine fraction removed) and fine fraction were minimal. Only very slight variations in the relative proportions of the major minerals present in each of these three fractions were indicated from XRD peak intensities. The most notable difference was observed between the sand fraction and whole rock; where it appears that the mica-phase and calcite decrease, while chlorite and albite increase. The differences in the XRD peak observations are summarised in Table 2. Figure 3 shows the XRD profiles for both the bulk diorite and the sand fractions, illustrating the magnitude of the differences.

Analysis of the fines reinforces the above conclusions, showing a complimentary relationship to the sand fraction (Table 3).

5.6.4 Geochemistry

Major and trace element analyses of the diorite starting material (MPG sample D337), both in terms of bulk rock and the sand fraction to be used in subsequent experiments, are presented in Table 3. Also given is the previously reported geochemical data for the diorite sample used in the Year 1 batch experiments (West *et al.*, 1997).

Some fractionation has occurred with removal of the 'fines' from the diorite starting material (MPG sample D337). Specifically, SiO_2, Al_2O_3 and Na_2O increase, while Fe_2O_3 (total), MgO and K_2O decrease, suggesting that the mafic mineral phases (biotite etc.) are concentrated into the fine fraction while felsic minerals (quartz and feldspars) are more resistant to crushing, and are concentrated into the sand fraction.

The whole rock geochemistry of the two samples (C853 & D337) is broadly similar. The most significant differences are in the oxides CaO and K_2O, LOI and the trace elements Rb and Ba. The greater LOI obtained for the diorite starting material (MPG sample D337) might suggest it was more altered, and it is noteworthy that all of the elements concerned are considered mobile during hydrothermal alteration and weathering (e.g. Wood *et al.* 1976).

5.6.5 Microorganisms

Microbial activity is of significance in the geochemical processes as it can influence mineral dissolution and precipitation, pH, alkalinity and redox status. Detailed studies into the subsurface microbiology of Äspö (Pedersen and Karlsson, 1995) had revealed the presence of many different bacteria in the granitic groundwater. Iron and sulphate reducing bacteria were highlighted as being of particular significance in Äspö geochemistry. The implications of iron reduction and sulphate reduction are discussed in detail in an earlier study (Banwart, 1995).

Studies previously undertaken by Goteborg University (Pedersen *et al.* 1996) had characterised an iron reducing isolate from the Äspö environment and had found it closely related to *Shewanella putrefaciens. S. putrefaciens* was therefore selected as the most representative iron reducing bacteria (IRB) for the study. *S. putrefaciens* uses ferric iron as an electron acceptor, in the process of iron reduction. It is a facultative anaerobe, able to use dissolved oxygen if available and to convert to anaerobic processes when it is absent. *S. putrefaciens* was obtained as a freeze-dried culture from Goteborg University.

The second microbe selected was a sulphate reducing bacteria (SRB), tentatively called *Desulfovibrio asponium.* Previous activity studies (Pedersen *et al* 1996) of bacterial samples from the Äspö environment, which looked at lactate utilisation and sulphide production, had indicated an SRB presence. DNA sequencing results had shown a close identity to *Desulfovibrio spp. D. asponium* was obtained from the German Collection of Microorganisms.

Desulfovibrio asponium (SRB) was first revived in Postgate B medium (Table 4) under anaerobic conditions at 30°C, and then transferred to Postage C medium (Table 4) and incubated under anaerobic conditions at 30°C. After successful growth in Postgate C medium, as determined by the presence of a turbid culture, a 10% inoculum was added to fresh Postgate C medium and incubated under anaerobic conditions on an orbital shaker at 30°C, and 200 rpm.

S. putrefaciens was received in a freeze-dried state. *Shewanella putrefaciens* was revived and incubated aerobically on an orbital shaker at 30°C and 200 rpm in Nutrient Broth (Oxoid, England). Solid medium plates of nutrient broth agar (Oxoid, England) were also used to maintain an active culture. After successful growth in nutrient broth, as determined by the presence of a turbid culture, a 2% inoculum was added to IRB medium (see Table 4) and incubated under anaerobic conditions on an orbital shaker at 30°C, and 200 rpm.

On obtaining a dense turbid culture, both cultures were harvested by centrifuging. The resulting cell pellets were re-suspended in anaerobic Äspö groundwater, and centrifuged at 13000 rpm for 10 minutes. This was repeated until the cells had been washed 2 times, after which time the cell pellets were re-suspended in 10 ml of anaerobic Äspö groundwater to form a dense cell paste for use in the inoculation of the experiments.

6. LABORATORY EXPERIMENTS

These experiments were designed to represent, as closely as possible (by using flowing systems so as to represent conditions that are more realistic), the reactions expected in the vicinity of the REX site and involved crushed potential host lithologies. In order to obtain information on the microbial effects on redox it is apparent that a fluid dominated system must be used. There are three basic types of experiments that may be used to investigate the rates of chemical reactions. Batch reactors, plug flow reactors and mixed flow reactors (Figure 4) have been studied and described by chemical engineers (Levenspiel, 1972; Hill; 1977).

In a batch reactor the reactants (fluids, solids, and bacteria) are initially charged into a container and allowed to reach equilibrium. Batch reactors are closed to mass flow. In a batch reactor, the composition of the reactants changes with time but at any one instant the composition throughout the reactor is uniform. These reactors were used for the initial (Year 1) investigations.

Plug flow reactors (or columns) are characterised by the orderly flow of fluid through the reactor moving parallel to the tube axis. Plug flow reactors are ideally operated in a steady state mode so that reactions can be studied under constant fluid composition conditions. This type of equipment was used for the Year 2 column investigations

The final type of reactor is the mixed-flow reactor or the continuously stirred tank reactor (CSTR). In this reactor, the contents are well mixed and uniform throughout, thus the exit stream from this reactor has the same composition as the bulk fluid within the reactor. CSTR systems are generally operated at far from equilibrium conditions to prevent the precipitation of secondary products. It was this type of reactor that were used in the Year 3 investigations

It was anticipated that the experiments would be conducted over a period of several months under an anaerobic atmosphere at a temperature of 30°C using Äspö groundwater. A series of experiments were conducted in which crushed Äspö Diorite was reacted with Äspö groundwater flowing into the system. Half the experiments were inoculated with a mixture of sulphate reducing bacteria and iron reducing bacteria (isolates from the Rock Laboratory) as previous experiments (West *et al*, 1997) have shown that they have an influence on fluid chemistry.

6.1 Flow through Column Experiments

The equipment (Figure 5) consisted of a fluid reservoir containing the Äspö groundwater connected via a peristaltic pump to the PEEK columns (30cm long, 0.7cm ID) which were connected in turn to the collection vessels (one per column). The whole apparatus was contained within an anaerobic chamber with a controlled nitrogen/hydrogen/carbon dioxide atmosphere. The Äspö groundwater was filter sterilised before use and the inlet end of the column contained a 0.2 μm filter in order to ensure that no other bacteria other than the SRB and IRB were present in the column. The outlet end of the column contained a 10 μm filter that was large enough for bacteria to pass through therefore enabling monitoring of bacteria that may be washed out of the column. The collection vessels were periodically changed and were sub-sampled for chemical, isotopic and microbiological analyses whilst still in the anaerobic chamber.

A total of eight column experiments (Table 5) were conducted under anaerobic conditions. Four of the columns contained only Äspö diorite reacting with Äspö groundwater. The remaining four columns contained Äspö diorite and mixed SRB and IRB cultures again reacting with the Äspö groundwater. The columns experiments were conducted in duplicate in order to obtain the maximum data from mineralogical observations

6.2 CSTR experiments

The equipment (Figures 6 and 7) consisted of a fluid reservoir containing the Äspö groundwater connected via a peristaltic pump to the Continuously Stirred Tank Reactors (CSTR) which were connected in turn to the collection vessels (one per reactor). The whole apparatus was contained within an anaerobic chamber with a controlled nitrogen/hydrogen/carbon dioxide atmosphere. As with the column experiments the Äspö groundwater was filter sterilised before use.

A total of four CSTR experiments (Table 5) were set up in an anaerobic chamber using 30g of crushed Äspö Diorite and 300 ml of sterilised Äspö groundwater. A mixed SRB and IRB culture of bacteria, isolated from the Äspö groundwater system, was injected into the vessels of two of the CSTR experiments (Run 1 and Run 2). The remaining two vessels were set up as abiotic controls. All four CSTR experiments were operated anaerobically for three months, after which two of the experiments (Run 1 and Run 4) were allowed to operate aerobically for a further three months.

The CSTR vessels were assembled in an anaerobic glove box ($H_2/CO_2/N_2$) at 30°C according to the following procedure: -

- All equipment was sterilised before assembly: the PTFE vessels and crushed Äspö Diorite were autoclaved and tubing and stirrer bars rinsed with methanol. The Äspö groundwater was sterilised by filtration through 0.2 μm filters.
- 30g of Äspö Diorite was then weighed into each of the four reaction vessels each of which contained a stirrer bar.
- Previously prepared active cultures of SRB and IRB bacteria were added to Vessels 1 and 2. Bacterial numbers had been determined using epifluorescence microscopy before transferring the cultures to the vessels.
- 300ml of sterile Äspö groundwater was added to each vessel which was then sealed and placed on top of a series of magnetic stirrers. The controls were adjusted to maintain continuous circulation of fluid within all four vessels.
- A reservoir of filtered groundwater was pumped into and out of the vessels, via a filter, to maintain a constant level of fluid.

After 100 days in an anaerobic chamber Vessels 1 and 4 were transferred to an aerobic atmosphere and continuously stirred at 30°C for the remainder of the experiment. The experiments in Vessels 2 and 3 were terminated at this time. Throughout the duration of the experiments, fluid was collected for chemical and microbial analyses. The flow rate of groundwater into the vessels and pH was also monitored. The reacted solids from the experiments were recovered on termination of the experiments and were stored in the anaerobic chamber until they before mineralogical and petrographic analysis.

6.3 Analytical techniques

6.3.1 Cryogenic scanning electron microscopy sample preparation

Solid residues from the column experiments were prepared for examination in wet-state under cryogenic conditions in the SEM (cryoSEM analysis). Analysis was performed using an Oxford Instruments CT1500 cryogenic preparation and transfer system fitted to a LEO 435VP variable pressure scanning electron microscope (SEM). Columns 6 (MPG sample No. D762, abiotic) and Column 2 (MPG sample No. D761, Äspö bacteria added) were initially frozen in liquid nitrogen

to physically fix the reacted residues in an ice glass. Subsamples were then cut from the frozen columns at the following intervals, measure with respect to distance from the column inlet:

(i) 0-2 cm,

(ii) 14-16 cm,

(iii) 26-28 cm.

The cut column sections were kept frozen in liquid nitrogen until analysis was performed. Experimental residues were extruded from the column sections and a sub-sample of the extruded material placed into a brass specimen holder. The specimen was then introduced to the cryogenic preparation unit for freeze fracturing before insertion into the SEM chamber. Within the SEM, the specimens were warmed to approximately 85°C to allow sublimation of the ice glass to reveal the specimen surface. After sublimation the specimen was cooled to less than -150°C and allowed to stabilise. The specimen was then returned to the cryogenic preparation unit and sputter-coated with gold. Coating was carried out in an argon atmosphere at 10^{-1} mbar with 20 mA current for 2 minutes.

Examination of the material from Column 6 (MPG sample D762, abiotic) revealed contamination of specimen surfaces with salts exsolved from the ice glass during solidification as described previously in the Phase 1 experiments (Wetton *et al.* 1998). In view of this a modified preparation procedure was adopted for Column 2 (MPG sample D761, Äspö bacterium added). The extruded material from the column section under analysis was allowed to thaw within the brass specimen holder. The specimen was then flushed three times using de-ionised sterile water. The specimen was then inserted into the cryogenic pre-freezing chamber and rapidly frozen in a solid nitrogen/liquid nitrogen melting mixture slush at about -196 °C. After freezing had occurred the slushing chamber was evacuated and the specimen transferred the cryogenic preparation unit (using a special vacuum-transfer device to prevent ice condensation on the frozen sample from atmospheric contact). Sample preparation from this point was identical to that described above.

6.3.2 Conventional scanning electron microscopy sample preparation

Samples for SEM analysis were initially subject to a rapid solvent replacement process (Fortin *et al.*, 1998) to remove the saline Äspö groundwater used in the experiments. A four stage dehydration was performed using solutions of 25, 50, 75 and 100% ethanol with each stage allowed to equilibrate for 15 minutes. The ethanol was then replaced by acetone in a two stage

process using 50%ethanol/50%acetone and 10% acetone. Following solvent replacement, a sub-sample was taken from each residue and allowed to air dry. The remaining residues were then retained under acetone for further analysis.

Portions of the air-dried material were mounted on 12 mm diameter aluminium pin-type SEM stubs using LEIT-C carbon-based electrically-conducting adhesive. The prepared stubs were coated with carbon by evaporation using an Emitech 950L turbo evaporator coater to give a coating thickness of approximately 25 nm.

6.3.3 Cryogenic SEM analysis

Solid residues from each experimental run were examined by cryogenic scanning electron microscopy (cryoSEM). Analysis was performed using a LEO 435VP variable pressure SEM fitted with an Oxford Instruments SEM cryogenic cold-stage. Identification of mineral surfaces under observation was aided by qualitative observation of X-ray spectra using an Oxford Instruments ISIS 300 EDXA microanalysis system. Further details of the analytical methods are described in Section 5.

Specimens were examined in the SEM under high vacuum and variable pressure conditions. Standard instrument conditions were 20 kV accelerating voltage and 75 pA probe current in high vacuum operation. Under variable pressure operation was performed in the range 0.1-0.3 torr as necessary to minimise charging at the specimen surface. SEM probe current and accelerating voltage under variable pressure operation were varied to obtain optimum imaging conditions. Preliminary examination of the specimens was performed before gold coating, using backscattered electron (BSE) imaging. This readily-allowed location of rare phases, e.g. pyrite, magnetite, sphene (titanite), etc., due to their high brightness under BSE imaging relative to the bulk background of the specimen. Stage positions were stored in the computer memory of the SEM for each grain found. This allowed their relocation after removal from the SEM for gold coating and subsequently, their re-insertion into the SEM for more detailed observation.

Initially, samples saturated with residual saline experimental fluid were examined directly by cryo-SEM. However, the precipitation of salt crystals from the fluid phase on freezing completely obscured the sample surfaces. Consequently, the cryo-SEM preparation was

modified by rinsing subsamples with distilled water, as described in Section 6.3.2 (above), in order to remove the saline pore fluid before cryo-SEM observation.

6.3.4 Conventional SEM analysis

The stub mounted samples were examined using a LEO 435VP variable pressure SEM operating under high vacuum conditions. The SEM instrument was operated at 20 kV accelerating voltage and probe currents of 75 to 350 pA in secondary electron imaging mode. Mineral identifications were aided by qualitative X-ray microanalysis, using an Oxford Instruments ISIS 300 energy-dispersive X-ray (EDXA) microanalysis system fitted to the SEM.

6.3.5 X-ray Diffraction Studies

X-ray diffraction (XRD) analysis of the starting material (MPG sample D337) is reported in Wetton *et al.,* (1998) and is therefore not discussed further. The fines fraction (< 5 μm) from both the column reactors and the stirred batch reactors were examined for compositional changes due to reaction. XRD analysis of the bulk residues from the experiments was not performed as SEM observations of the residues showed evidence of very limited levels of reaction, which would be beyond the sensitivity limits of the XRD technique.

Residues were received under acetone and each was sub-sampled retaining a 50 % split for reference purposes or further analysis. The material taken for XRD analysis was initially dried to remove the acetone content and then re-dispersed in 75 ml of deionised water. This was then subject to ultrasonic dispersion for approximately 3 minutes. The resulting suspension was then sieved on a 63 μm mesh, and the < 63 μm fraction extracted. This fraction was then placed in a 100 ml measuring cylinder to allow sedimentation of the material. A nominal < 5 μm suspension was removed from the measuring cylinder after a settling time as dictated by Stokes Law and concentrated by centrifuging. Concentrates from the centrifuging process were pipetted onto frosted glass slips to produce orientated mounts that were allowed to air dry.

XRD analysis was carried out using a Phillips PW1700 series diffractometer using CoK_ radiation and operating at 45 kV and 40 mA. The orientated mounts were scanned over the range 1.5 to 32 2θ at a scanning speed of 0.5 2θ/minute. Scans were performed on the slips in the original air-dried state and as ethylene glycol solvated mounts to assist the clay mineral identifications. Diffraction data were analysed using Phillips X'Pert software coupled to an International Centre for Diffraction Data (ICCD) database running under Windows NT4.0.

6.3.6 Chemical analyses

Chemical analyses included major anions and cations; trace elements; redox sensitive species including FeII/FeIII, $NH_4/NO_3/N_2O$, $SO_4/S_2O_3/H_2S$, As^{III}/As^{V}, Se^{IV}/Se^{VI} and selected microbial nutrients (e.g. C, O, N, P). Each of the sampled fluids was split into several subsamples. A sub-sample of 1 ml was taken for immediate analysis of pH using an Orion 520 pH meter, fitted with a Whatman glass combination electrode calibrated at room temperature with NBS traceable buffers at pH 7 and 10. Cations were determined by inductively coupled plasma-optical emission spectrometry (ICP-OES). Anions were determined by Ion Chromatography (IC). A further sub-sample was complexed to 0.1% with respect to 2,2-bipyridyl, this was used for the determination of reduced iron by colorimetry using a Phillips PU 8740 scanning UV/visible spectrophotometer. Another sub-sample was taken and preserved with respect to NaOH solution and used for the determination of reduced sulphur by Hydride Generation Inductively Coupled Plasma-Optical Emission Spectrometry (HGICP-OES).

6.3.7 Microbiological analyses

A sub-sample of 1 ml was taken for microbiological analyses to which was added a fixative solution in order to prevent any deterioration of the bacteria prior to staining. Glutaraldehyde is a commonly used fixative for bacterial samples - whilst respiration ceases, the cells retain their original morphology. 1ml of sample was added to a 10ml solution of 0.5% gluteraldehyde in cacodylate buffer and stored in the dark at 4%C (Jass & Lappin-Scott, 1992).

The numbers of bacteria present in the groundwater was assessed using a total count method of epifluorescence microscopy (Hobbie *et al.*, 1977). This method is based upon a light source transmitting short wavelength radiation onto a specimen that has been filtered and retained on a membrane. The specimen is first stained with a fluorochrome solution, acridine orange, which interacts with the nuclear material of the bacteria and emits longwave radiation. When the membranes are viewed under the microscope the bacteria appear as bright green and red fluorescing cells against a dark background which enables them to be counted. By examining 20 randomly selected fields of view, individual numbers can be counted and the number of bacteria per ml of sample determined. The staining procedure is detailed in West *et al* (1997) and West (1998).

Selected samples were also analysed using FAME analysis (fatty acid methyl ester analysis). This technique analyses fatty acids present in the bacteria cell membranes, which can provide a means of identifying bacteria due to the unique chemicals in their membranes. The samples are first dissolved in chloroform: methanol solution to extract the lipids from the microbial membranes, which are then analysed by gas chromatography. The fatty acids separate in the gas chromatograph based on their molecular weight and boiling point. This then provides a 'fingerprint' that can be compared to previously determined standards of known microorganisms.

6.3.8 Stable isotope analyses

In anoxic reducing environments at normal earth surface temperatures, bacterial sulphate reduction is one of the most prominent processes. This biologically mediated process can have profound effects on the chemistry of fluids and fluid: rock reactions. One of the diagnostic features of this process is the large fractionation between the isotopic composition of sulphur in the original dissolved sulphate and that of the sulphide produced. Generally in natural systems the fractionation associated with bacterial sulphate reduction is relatively constant $\alpha = 1.003$ (Goldhaber and Kaplan 1974). With progression of the reaction, the isotopic ratio of the residual sulphate increases. Due to the large fractionation factor, this increase is rapid, with respect to the amount of sulphate consumed. The alternative approach, namely to analyse (using chemical methods) the produced sulphide may not be successful if the produced sulphide undergoes further reactions.

The rationale for the inclusion of sulphur isotope fractionation analysis in this study is that the $\delta^{34}S$ of the residual sulphate or rather the deviation of the $\delta^{34}S$ of the residual sulphate from that of the initial sulphate can provide a measure of the extent of the reduction process.

Aliquots of the fluid were taken at regular intervals for chemical and isotopic analysis. The concentration of sulphate in the collected fluids was sufficiently high for the use of the standard procedure for sulphate precipitation. The individual 50ml water sample aliquots were acidified with 0.1M HCl and brought to boiling. A 6% $BaCl_2$ solution at an estimated 5 fold excess was added while stirring. Boiling was discontinued and the precipitate formed was allowed to age overnight. The $BaSO_4$ precipitate was prepared for sulphur isotope ratio determination from SO_2

using the method of Coleman and Moore (1978). Analysis was carried out using a VG SIRA 10 Mass spectrometer.

6.4 Experimental Results

The column experiments were run for about two weeks before the columns with bacteria added became blocked and flow fluid ceased. Two of the columns – Column 2 (bacteria added) and a control, Column 6 (no bacteria) – were examined to investigate any mineralogical changes that had occurred. All four CSTR experiments were operated anaerobically for three months, after which two of the experiments (Run 1 and Run 4) were allowed to operate aerobically for a further three months. All four CSTR experiments were examined to investigate any mineralogical changes that had occurred.

6.5 Mineralogical Results

A summary of all samples analysed and the relevant analytical techniques are presented in Table 6.

6.5.1 Conventional SEM observations

(a) Crushed diorite starting material – D337

The mineralogical and petrographic characteristics of the crushed Äspö Diorite starting material are described in detail by Wetton *et al.* (1998). SEM observations showed that a significant amount of fine grained (< 2 μm) material (derived from the crushing processes) was present on mineral grain surfaces despite the rigorous crushing and cleaning performed on the material (Wetton et. al, 1998). The bulk of this fine grained material was seen to adhere to the surfaces of the grains in the 125-250 μm size fraction. The fines have a typical Äspö Diorite mineralogy, being primarily composed of albite, orthoclase, chlorite/chloritised mica, and have angular and irregular morphologies consistent with their formation by mechanical crushing. Typical fines morphologies and concentrations are illustrated in Plates 1 and 2.

Quartz grains within the crushed material show a mixture of smooth and conchoidal fracture surfaces, with sharp grain edges formed by the crushing process. Grain surfaces are typically coated with fine grained mineral material, with enhanced concentrations of fines being trapped in the irregularities within concave and stepped areas of the grain surface (Plate3). Alkali feldspar within the material was identified as mainly albite by EDXA, though some grains showed

considerable Ca content suggesting a component of more calcic plagioclase may be present. Albite grain surfaces displayed morphologies ranging from simple smooth surfaces (showing relict imprints or 'moulds' of originally adjacent contacting grains) to irregular 'stepped' morphologies where grains exceeding the 125-250 μm target size had fractured along cleavages during the crushing process. Orthoclase feldspar grains observed in the sample tended to show primarily stepped and irregular forms.

Biotite and chlorite/chloritised biotite in the sample showed mechanical distortion, with folding of mica sheets at their grain edges (Plate 4), and minor 'splaying' along the basal cleavage plane. Some evidence of corrosion along the basal cleavage of splayed mica grains was observed, possibly indicating minor in situ dissolution of the mica sheets prior to the sampling exercise. All grain surfaces show fines present, with some fines having penetrated along open/splayed cleavage planes (Plate 5). Calcite grains were observed in the sample, as compound grains often intergrown with albite or quartz. Contrasting surface textures were observed on the calcite grains ranging from highly corroded (Plate 6) to near pristine crystal faces (Plate 7). Accessory mineral phases observed included sphene (titanite), hornblende, magnetite and pyrite. In all cases, these grains showed no evidence of prior in situ reactions or high surface concentrations of fine particles.

(b) Column residues

Conventional SEM observation of materials from the columns experiments was not performed, as is was not possible to wash the samples to remove the Äspö ground water since the columns had become blocked, instead cryoSEM was performed (Section 6.4.2).

(c) CSTR experiment materials

Anaerobic experiments

SEM observation of materials from the anaerobic CSTR experiments showed only minor differences between the bacteria added experiment, CSTR Run 2 (MPG sample D285), and the abiotic control CSTR Run 3 (MPG SAMPLE D286). Analysis of sample CSTR Run 2 (MPG sample D285) showed no evidence, nor preservation, of any biofilm structures, nor any evidence for the presence of the bacteria which had been added to experiment. In addition, with the possible exception of the biotite and calcite components, no reaction could be observed in the major or accessory minerals present in the diorite. Biotite mica did show some possible

evidence of minor dissolution at plate edges and increased exfoliation of grains, Plate 8 - CSTR Run 2 (MPG sample D285) and Plate 9 - CSTR Run 3 (MPG sample D286), but no difference could be observed between the two experimental conditions. Etching of calcite grains was observed in both anaerobic experiments with typical textures shown in Plate 10. In both experimental residues, grain surfaces showed a marked decrease in the concentration of fine particles present. This may indicate preferential reaction of the fine particles as a result of their relatively high reactivity due to high surface area in comparison to grains from the 125 to 250 μm size range. In the experiment, which included the bacteria, fine grained mineral phases were infrequently observed particularly on quartz grain surfaces (Plate 11). EDXA indicated possible clay compositions (Al and Si dominated) for some of these whilst others showed only Ca and S present indicating possibly gypsum.

Anaerobic-aerobic experiments

Examination of the anaerobic-aerobic experiment residues showed similar features to those seen in the anaerobic experiments. The bacteria-added experiment, CSTR Run 1 (MPG sample D284), showed no evidence for the development or preservation of biofilm structures, nor any evidence of bacteria within the sample. Loss of fine particles from the grain surfaces relative to the starting material was clearly evident in both samples, but reaction of the 125 to 250 μm fraction grains was not observed. Biotite and calcite (calcite was only observed in the abiotic experiment, CSTR 4) show tentative evidence of reaction, though the range of textures observed differ very little from those seen in the starting material. Formation of fine grained material, previously identified as gypsum in sample CSTR Run 2 (MPG sample D285), was evident as fine mats of crystals in sample CSTR Run 4 (MPG sample D287), the abiotic anaerobic-aerobic experiment (Plate 12). Fine grained material with Na-K-Al-silicate type compositions was observed in association with the gypsum. The presence of gypsum in three of the experimental residues suggests it to be a precipitate from the experimental fluid not removed during sample preparation. This implies that the pyrite present in the starting material had been oxidised to form sulphates.

6.5.2 CryoSEM observations

(a) Column residues

Observations from the Column 6 (MPG sampleD762, abiotic) experiment were very limited because of the high volumes of salts precipitated from the experimental fluid during cryogenic preparation (Plate 13), which obscured any detail of the mineral surfaces. Where observations of grain surfaces were made no clear evidence of dissolution or precipitation of minerals was found.

SEM examination of Column 2 (MPG sampleD761, Äspö bacteria added) allowed some observations to be made, as salt precipitation was greatly reduced by using the modified cryoSEM preparation method described in Section 6.3.3. Salt contamination where present was now observed as clusters of individual precipitates (Plate 14) rather than surface coating films as seen in the previous column. Grain surfaces at the column inlet, (MPG sub-sample D761C1, 0 to 2 cm), showed no evidence of mineral dissolution or precipitation. Structures tentatively identified as organic filaments (possibly corresponding to polysaccharide filaments or biofilm) were observed on some grain surfaces, entrapping fine grained Äspö Diorite fines and possible smectitic or chloritic clay-like silicate mineral material (Plate 15). Significant amounts of fines appear to have been mobilised from the grain surfaces during the course of the experiment. The filaments appeared to have trapped fines as they have moved through the pore-throats of the crushed Äspö Diorite material packing the columns, consequently blocking or restricting the porosity.

Similar observations were made on sub-samples from 14-18 cm (MPG sub-sample D761C3) and 26-28 cm (MPG sub-sample D761C2) from the column inlet. However, much of sample (MPG sub-sample D761C2) was still obscured by salts precipitated from residual saline porewater, which had not been completely removed during sample preparation. Consequently, the filamentous 'biofilm' was seen to be heavily encrusted with NaCl crystals. Fine, smectite-like clay appeared to have grown on the surfaces of some grains during the course of the experiment (Plate 16).

(b) CSTR experiment residues

Cryo-SEM was not performed on these samples as the conventional SEM observation of materials showed only minor differences between the experiments.

6.5.3 XRD analysis

(a) Column residues

The fine (nominal <5 μm size) fraction was separated from the residue of Column 2 (Sample D761) and analysed by XRD as an orientated mount. The XRD results were compared with those obtained from fine fraction separated from the original Äspö Diorite starting experimental feedstock material. XRD indicated that a chlorite-smectite/smectite phase was present in the fine fraction of the experimental residue. This had a characteristic diffraction peak corresponding to a d-spacing of 14.9 Å (Figure 8), which increased on glycolation. This phase was absent in the original starting material (Figure 8) and, therefore, must have formed as a reaction product during the course of the experiment.

(b) CSTR experiment residues

XRD analysis of the fine (< 5 μm) fraction of the experimental residues showed that significant mineralogical changes had occurred in all experimental residues relative to the fine fraction of the original Äspö Diorite starting material. Figures 9a and 9b compare the XRD traces obtained for the residue fine fractions from the aerobic (biotic and abiotic) and anaerobic (biotic and abiotic) experiments, respectively. Figures 10a and 10b compare the XRD traces of aerobic and anaerobic experimental residues, with and without bacteria, respectively.

The fine fraction residues all show the presence of a XRD peak at 14.45 Å (7.1° 2θ, Figure 9a,b; Figure 10a,b) corresponding to smectite. This is absent in the starting material (Figure 8) and must therefore have formed during the experiments. However, there is a significant difference in the amount of smectite formed (as indicated by the size of the XRD peak) between the abiotic and biotic experiments. Fine fractions of the residues from the experiments containing Äspö bacteria, CSTR Run 1 (MPG sample D284) and CSTR Run 2 (MPG sample D285), showed a smectite species present as a major component. Residues from experiments without Äspö bacteria show the development of significantly less secondary smectite.

The XRD data clearly indicate that interaction with the Äspö groundwater has caused reaction of the chlorite in the starting material to form smectite products, probably via the development of smectite interlayers within the chlorite from the original starting material. The extent of this reaction appears to be strongly enhanced in the experiments where bacteria were present. Smectite formation shows little variation with experimental conditions, whether anaerobic only or anaerobic-aerobic.

6.5.4 Microbial observations

Table 7 and Figure 11 show the results of bacterial enumeration by epifluorescence microscopy. During the anaerobic incubation period, the number of bacteria in vessel 1 showed a steady decline from 2.43×10^5 to 4.9×10^3 per ml of fluid. Bacteria in vessel 2 also reduced in number although at a slower rate from 2.43×10^5 to 6.57×10^4 per ml of fluid. This decline in numbers suggests they are able to survive for a limited period but there is a limiting factor or factors affecting their growth. Vessels 3 and 4 both remained relatively sterile up to 94 days incubation with numbers of bacteria detected at <50 per ml of fluid.

After 15 days in an aerobic atmosphere (115 from experiment set-up), vessels 1 and 4 were sampled for microbial analyses and bacterial numbers were shown to have greatly increased in both vessels. In vessel 1, the number of bacteria had increased from 4.9×10^3 to 1.63×10^6 per ml of fluid.

In vessel 4 the number of bacteria had increased from <50 at 94 days in anaerobic incubation to 7.62×10^3 at 2 days and 4.68×10^5 after 15 days in an aerobic atmosphere. Since vessel 4 had previously been sterile, further investigations were carried out in order to determine the source of the bacterial contamination. This would also determine the likely cause of the increase in numbers found in vessel 1.

Analysis of the isolated microbiological contaminants indicate that the most likely cause of the microbiological contamination of the CSTR experiments was due to ingress of microbes into the reservoir of groundwater used to feed the CSTR, and directly into the CSTR.

Results from the FAME analysis confirm results obtained during the experiment, that both *Shewanella putrefaciens* (IRB) and *Desulfovibrio asponium* (SRB) are not present in the reactors

after the anaerobic phase of the experiment. It should be noted that some of the isolates were not identified.

At the end of the experiment (182 days) bacterial numbers in vessel 1 had decreased from 1.63 x 10^6 per ml of fluid at 115 days to 5.49 x 10^4. In vessel 4 the number of bacteria had decreased from 4.68 x 10^5 per ml of fluid at 115 days to 2.36 x 10^4.

Although the vessels had become contaminated during the course of the experiment, the results had shown that the Äspö Diorite and groundwater were capable of supporting a bacterial population at 30°C.

6.5.5 Chemical analyses results

A full listing of the chemical analysis data for all the experimental fluids can be found in Tables 8 to 13, all data has an associated analytical error of 5%. The following discussion of the chemistry of the experimental fluids is concerned with differences between the starting fluid composition and the experimental fluid chemistries.

As the columns experiments ran for only a short time data is limited (Tables 8 and 9), the CSTR experiments however ran for several months and full analytical data (Tables 10 to 13) is available. Little evidence for rock-water interactions is seen in the chemical analysis data for both the columns and the CSTR experiments. There are some slight initial increases observed for some elements (i.e. Si, Al) but this is probably the result of the re-establishment of equilibrium between the ground water and the crushed rock as no further trends are observed. However, the data suggests that there has been some limited dissolution of primary minerals present in the rock. This is in agreement with the mineralogical observations. Examination of the saturation state of the fluids showed them to be saturated with respect to clay minerals. Possibly, the observed mineralogical changes reflect alteration occurring in microbially mediated microenvironments close to mineral surfaces. Consequently, these changes may be too small to be detected in the chemical analysis of the bulk fluid.

Several chemical parameters may indicate bacterial sulphate reduction, the sulphate concentration (Tables 10 to 13) remains relatively constant, throughout the experiments, within the analytical error for sulphate determination. The sulphide concentration fluctuates and seems

to be a rough indicator for the redox conditions in the system, however in most cases the levels of reduced sulphur are not more than 3 times detection limit therefore the reliability of this indicator is not very good. The TOC decreases in all experiments, while the trend of TIC is roughly antipathetic but correlation is not strong. Therefore, it is not possible to determine whether or not there is a significant difference between the experiments with and without bacteria in the oxidation of organic to inorganic carbon. It is important to notice that in the first fluid sample of all experiments the contents of TOC and TIC are much higher than in the starting fluid. This suggests that both organic and inorganic carbon are derived from the solid. Similarly, the level of Zn and Cu are also lower in the starting fluid than in most fluid samples taken in the course of the experiment. The first fluid samples have the highest concentration of these metals and they show an overall decrease with the progression of the experiment. This could be due to progressive leaching or to precipitation of metal sulphides.

6.5.6 Stable isotope results

The results of the stable isotope analysis are given in Table 14 and are expressed as δ^{34} S as permil (‰) deviation from the VCDT standard with an overall analytical reproducibility of ±0.1‰. Reference materials IAEA-S-1 gave -0.3‰ and NBS122 gave 0.15‰.

The sulphur isotope composition of the starting fluid (8.3‰) is the lowest value recorded throughout the experiment. In view of the high sulphate concentration it seems that the sulphate in the starting fluid may be acquired from sedimentary rocks, however this remains uncertain. An increase in this value could be an indicator for the process of sulphate reduction. Experiments conducted with bacteria (vessels 1 and 2) show a systematic increase in δ^{34}S from a starting value of 9.8 to 11.4‰ when the experiments turned aerobic. This increase was not recorded in the experiments conducted without bacteria (vessels 3 and 4). These trends coincide roughly with the increase in reduced sulphide in vessel 1. It should be noted however that high levels of reduced sulphur were recorded in vessel 4.

In summary: the changes in δ^{34}S of dissolved sulphate in the experiments with bacteria suggest that bacterial sulphate reduction indeed occurs. However, the constantly high concentration of sulphate in the fluid prevents a quantitative assessment of this process.

7. DISCUSSION

7.1 Mineralogy and Petrology

The experimental residues generally show only limited evidence of mineralogical alteration relative to the starting material. Although some evidence of biofilm development was observed during SEM analysis of residues from the column experiments, the CSTR experiments showed no clear evidence (or preservation) of biofilm development, or of bacteria present in the samples. SEM observation of the chloritised micas however shows no significant evidence for reaction of the sand-grade grains from the experimental residues when compared to the starting material. SEM observations show a loss of fine grained, <5 μm, material which adheres to grain surfaces in the starting material. There is also evidence for the formation of very minor amounts of secondary smectite-like clay mineral precipitates on grain surfaces. Mineralogical changes, detected by XRD analysis of the fine-fraction also provide evidence of mineral reaction during the course of the experiments. Minor conversion of chlorite and chloritised biotite fines present within the crushed diorite has produced smectite and chlorite-smectite interlayers. The degree of alteration appears to be very significantly enhanced by the presence of the Äspö bacteria, but no difference in reaction is seen between the anaerobic experiments, and the experiments which were initially anaerobic and subsequently run aerobically for a further three months. This would suggest that most of the smectite formation occurred during the first three months of the experiments, when all four experiments were run under anaerobic conditions. Subsequent operation of two of the experiments for a further three months under aerobic conditions appears to have had no further effect on the alteration products observed.

In this respect, the observations are consistent with those on the column experiments. The columns with bacteria very rapidly became blocked (after only a few days of operation), and minor amounts of smectite was observed in the reaction residues examined after this period. Experiments without bacteria did not block up. Thus, it would appear that bacterially-enhanced smectite formation might have been partially responsible for the blocking of the column experiments.

The absence of bacteria and bacterially derived structures in the samples is a matter of concern as bacterial populations using epifluorescence microscopy indicate populations around 10^6

bacteria/ml. This suggests that preparation of the experimental residues is effectively removing all bacteria and any biologically derived material resulting from their presence. Post analytical discussions with microbiology laboratory staff indicate that the washing process used during preparation of the cryo-SEM specimens would be extremely detrimental to the condition of any bacteria and biofilms present. This is due to the large difference in solute concentration between the Äspö groundwater used in the experiments and the de-ionised water used for flushing. This could lead to large osmotic pressure differences across bacterial membranes causing them to rupture. The failure to preserve bacteria in the materials prepared for conventional SEM is of more concern. During the solvent replacement process, no provision was made to reclaim fine grained material, which may have become suspended in the fluid during the solvent exchanges. This may have led to any bacteria present and a large proportion of the fine grained material being lost from the samples. These problems highlight the need for development of expertise in the preparation of biological specimens for SEM analysis. Additionally the experimental design process must include consideration of the analytical methods that are to apply to the experimental products. The high-energy environment of a stirred reactor system may offer enhanced reaction rates for mineral dissolution/precipitation but may be detrimental in microbially driven processes. Continual contacting of grain surfaces during stirring and the relatively high fluid flow rates apparent at grain surfaces may prevent biofilm development and hamper bacterial adhesion. Prior studies of the Äspö bacteria (Pedersen *et al.* 1996) have produced successful characterisations using sterile glass sections immersed into the Äspö groundwater system.

7.2 Microbiology

Although the vessels had become contaminated during the course of the experiment, the results had shown that the Äspö Diorite and groundwater were capable of supporting a bacterial population at 30°C. To minimise contamination in future experiments, strict aseptic technique should be employed and appropriate microbiological fermentation methods used in the construction and maintenance of reactors.

7.3 Chemistry

Fluid chemical analysis shows little evidence for rock-water interactions is seen in the chemical analysis data for both the columns and the CSTR experiments. There are some slight initial increases observed for some elements (i.e. Si, Al) but this is probably the result of the re-

establishment of equilibrium between the ground water and the crushed rock as no further trends are observed. It is worth noting, in the light of the mineralogical changes observed, that the chemical analysis is representative only of the bulk fluid composition and that any changes in fluid chemistry occurring in microbially mediated microenvironments close to mineral surfaces may be too small to significantly effect the bulk fluid.

7.3.1 Stable isotopes

The changes in $\delta^{34}S$ of dissolved sulphate in the experiments with bacteria suggest that bacterial sulphate reduction indeed takes place. However, the constantly high concentration of sulphate in the fluid prevents a quantitative assessment of this process.

8. CONCLUSIONS

The residues from the different types of experiment undertaken all show only very limited evidence of mineralogical alteration relative to the starting material. In most cases, it is the very fine grained (<2 μm) comminuted material, produced by crushing of the Äspö Diorite starting material, which has reacted preferentially. A significant amount of this fine material remained adhered to the coarser grain surfaces of the experimental charge material, despite attempts to remove it by washing and ultrasonic treatment. XRD showed that this fine material is mineralogically similar to the bulk of the starting material. Its reactivity is attributed to its high surface area.

There is petrographic (SEM) evidence for the formation of very minor amounts of secondary smectite- or chlorite-smectite-like clay nucleation on grain surfaces. Mineralogical changes, detected by XRD analysis of the fine fraction also provide evidence of mineral reaction during the course of the experiments. Minor alteration of chlorite and chloritised biotite fines present within the crushed diorite has resulted in the production of smectite and smectite interlayers in the 'primary' phyllosilicates. Although the fluid phase was saturated with respect to smectite solubility in all of the experiment, the amount of smectite formed appears to be very significantly enhanced by the presence of the Äspö bacteria. Possibly, the bacteria catalyse the growth of smectite, perhaps by acting as favourable sites for nucleation. The local site chemistry of bacterial cell surfaces or associated biofilm may create a microchemical environment that speeds the kinetics of clay nucleation, or may present suitable template surface for clay nucleation. Additional research is required to confirm whether the hypothesis of bacterially enhanced smectite formation is correct. If bacterial action is indeed shown to be responsible for the enhanced rate of smectite formation, then the mechanism needs to be established by further work.

8.1 Relevance to radioactive waste research investigations in Japan

Although the REX laboratory experiments were built around the use of Swedish Äspö Diorite, the results of these experiments have direct relevance for issues concerning redox buffering in radioactive waste disposal problems in Japan. The mineralogy of the Äspö Diorite comprises major quartz, plagioclase (albite), orthoclase, biotite, and hornblende, with trace amounts of minerals such as titanite, apatite, sulphides (e.g. pyrite, chalcopyrite), Ti-Fe oxides and

secondary alteration products such as chloritised biotite, chlorite, epidote, calcite, sulphides, fluorite, sericite and hematite. Similar mineral assemblages are found in rocks that are the focus of radioactive waste research in Japan (e.g. Tono Granite, Kamaishi Granodiorite). Therefore in these rocks, it is possible that mineralogical alteration in low-temperature groundwater systems will be similarly influenced by microbial processes.

8.2 Implications for permeability

The REX laboratory experimental study has clearly demonstrated that despite the small amount of geochemical/mineralogical alteration that occurred, microbial activity can have a significant impact on the transport properties of the rock mass. The experimental columns influenced by bacteria rapidly became blocked due to the formation of biofilms, which trapped fines migrating through the intergranular porosity. This, together with the preferential formation of pore-lining smectite in the biologically active experiments, resulted in major reduction in permeability, although volumetrically, very little alteration had occurred. In a more nutrient-rich or organic-rich environment (the "Äspö Diorite environment" experiments were low in nutrients) the effect would be expected to be much greater because biological activity would be expected to be greater. By analogy, similar processes might be expected to occur in the environment around a repository. The development of biofilms would potentially lead to the trapping of colloidal particles or fine-grained material migrating through fractured rock or porous rock flow systems, leading to a narrowing of pore throats and reduction in flow. The permeability may be further reduced, if clays such as smectite were encouraged to nucleate within the pores as a result of microbial activity. The encouragement of the formation of secondary smectite, by bacterial activity, also has important implications for radionuclide sorption. Smectite has high surface area and strong ion-exchange properties. Its formation could result in an increase in the retardation properties of the rock mass for certain radionuclides as a result of increased sorption and ion-exchange.

9. REFERENCES

Banwart, S. (editor). 1995. The Äspö Redox Investigations in Block Scale. Project summary and implications for repository performance assessment. *SKB Technical Report*, **95-26**.

Coleman M.L. and Moore M.P. 1978. Direct reduction of sulphates to sulphur dioxide for isotopic analysis. Anal. Chem. 50 1594-1595.

Fortin, D., Grant Ferris, F. and Scott, S.D. 1998. Formation of Fe-silicates and Fe-oxides on bacterial surface in samples collected near hydrothermal vents on the Southern Explorer Ridge in the northeast Pacific ocean. *American mineralogist*, 83,1399-1408.

Goldhaber M. B. and Kaplan I. R. 1974. The sulphur cycle. In Goldberg E.D. (Ed) The sea Wiley, New York, pp 569-656

Hill, C. G. 1977 An Introduction to Chemical Engineering Kinetics and Reactor Design. John Wiley and Sons New York.

Hobbie, J. E., Daley, R. J. and Jasper, S. 1977. Use of Nucleopre Filters for Counting Bacteria by Fluorescence Microscopy. Applied and Environmental Microbiology, 33, (5), 1225-1228.

Jass, J., and Lappin-Scott, H.M. 1992. A Practical Course on Biofilm Formation Using The Modified Robbins Device. Biofilm Technologies Research Group, University of Exeter, England. pp. 1-34

Landström, O. and Tullborg, E-L. 1995. Interactions of trace elements with fracture filling minerals from Äspö Hard Rock Laboratory. *SKB Technical Report*, **95-13**.

Levenspiel, O. 1972 Chemical Reaction Engineering (2nd Edition) John Wiley and Sons. New York.

Milodowski, A. E., Gillespie, M. R., and Yoshida H. 1996. Mineralogical logging and characterisation of flowing features in the two REX boreholes KA2858A and KA2862A, Äspö

hard rock laboratory, southeastern Sweden. *British Geological Survey, Technical Report,* **WE/96/15C.**

Pedersen, K., and Karlsson. 1995 Investigations of Subterrean Microorganisms. Their importance for performance assessment of radioactive waste disposal. SKB Technical Report 95-10. Stockholm.

Pedersen, K., Arlinger, J., Ekendahl, S., and Hallbeck, L. 1996. 16S ribosomal-RNA gene diversity of attached and unattached bacteria in boreholes along the access tunnels to the Äspö hard rock laboratory, Sweden. *Fems Microbiology Ecology*, 19, No. 4, 249-262.

West, J. M. Aoki, K., Baker, S. J., Bateman, K., Coombs, P., Gillespie, M. R., Henney, P. J., Reeder, S., Milodowski, A. E. and Yoshida, H. 1997 Complementary laboratory work to examine microbial effects on redox and quantification of the effects of microbiological perturbations on the geological disposal of HLW (TRU). Task 1. Äspö Hard Rock Laboratory - Redox Experiment in detailed scale (REX). *British Geological Survey, Technical Report,* **WE/97/3C.**

West, J.M. (editor). 1998. A Three Task Project: Task 1. Laboratory work to examine microbial effects on redox and quantification of the effects of microbiological perturbations on the geological disposal of HLW (TRU); Task 2. Geochemical profile through the Tsukiyoshi Fault Zone; Task 3. Presentation of Year 1 results at international conferences. *British Geological Survey, Technical Report,* **WE/98/11C.**

Wetton, P.D., Milodowski, A.E. and Hards, V.L. 1998. Redox experiment in detailed scale (REX). Complementary laboratory studies to examine microbial effects on redox in a high-level radioactive waste repository: Mineralogical characterisation of residues from Year 1 batch experiments, and sampling and analysis of Year 2 column experiments. **WG/98/1C (Issue 1)**

Winberg, A., Andersson, P., Hermanson, J. & Stenberg, L. 1996. Results of the Select Project: investigation programme for the selection sites for the operational phase. *SKB Swedish Hard Rock Laboratory Progress Report,* **HRL-96-01.**

Wood, D A, Gibson, I L & Thompson, R N. 1976. Elemental mobility during zeolite facies metamorphism of the Tertiary basalts of Eastern Iceland. *Contributions to Mineralogy and Petrology*, **55**, 241-254

10. ACKNOWLEDGEMENTS

Chemical Analyses:

M. Cave, S. Reeder, P Blackwell, S. Chenery, M. Ingham, J. Trick, J. Wragg

Administration, QA Procedures and Report Preparation:

C. Cole, J. Mackrill, Y Moore

Financial administration:

L. Riley, C. Connett

This work is published with the permission of the Director of the British Geological Survey.

Figures

Figure 1 Location of the Äspö Hard Rock Laboratory (from Landstrom and Tullborg, 1995)

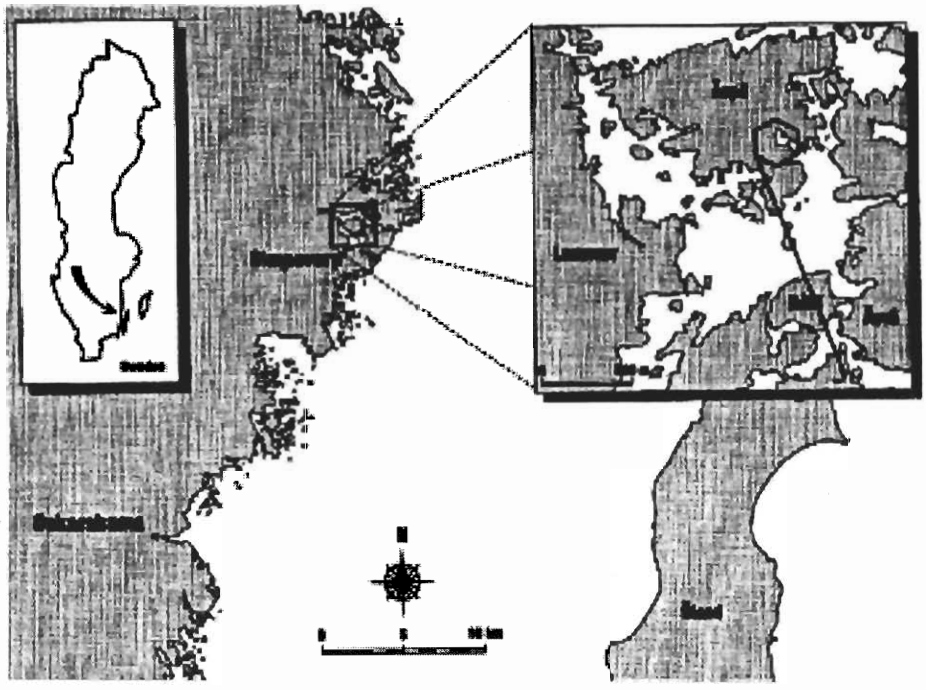

Figure 2 Summary of structural elements of the REX block (from Winberg *et al*, 1996)

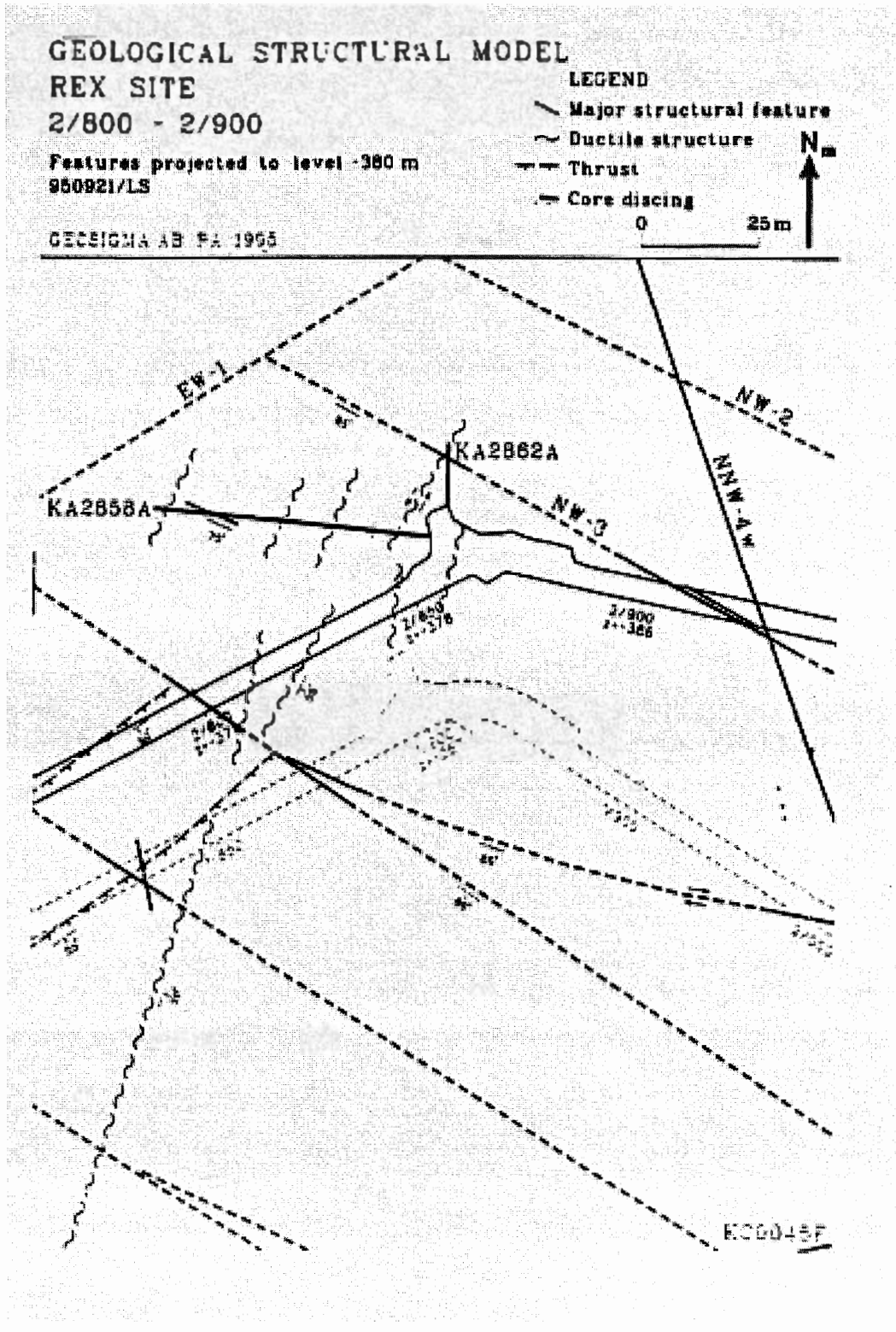

Figure 3 Diorite starting material; overlain X-ray diffraction (XRD) profiles for comparison of mineralogical differences between prepared sand fraction (black) and original bulk diorite (red)

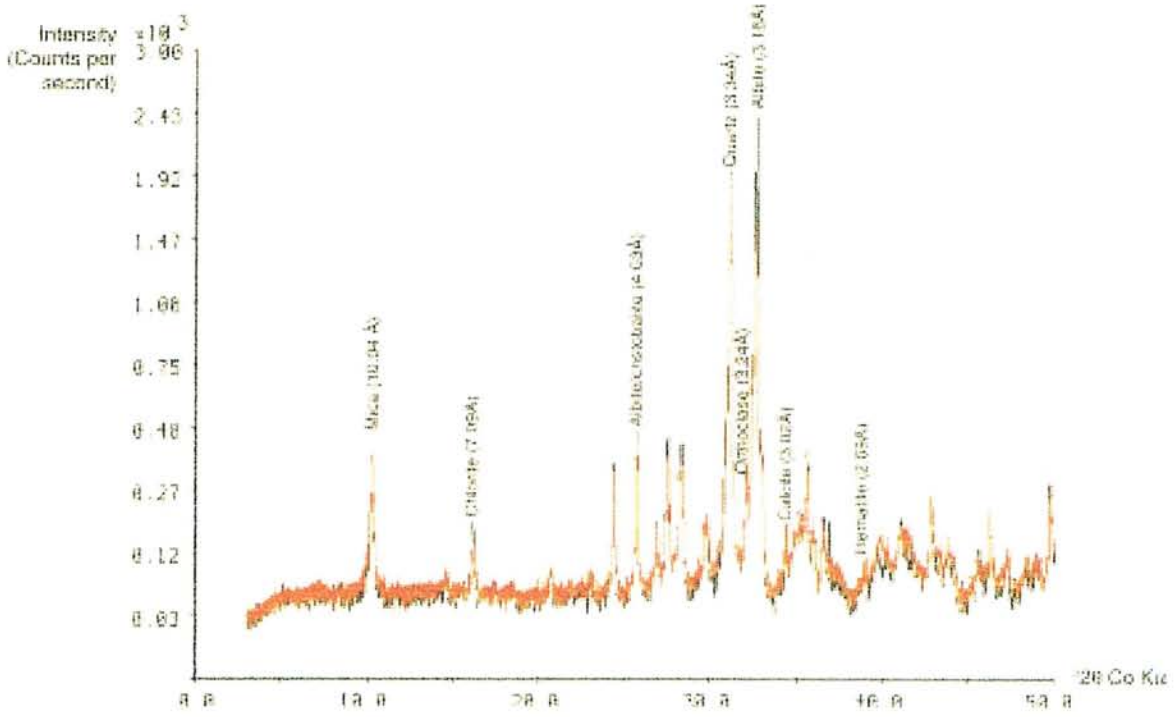

Figure 4 The three types of reactors: (a) batch reactor, (b) columns and (c) continuously stirred tank reactor (adapted from Levenspiel, 1972)

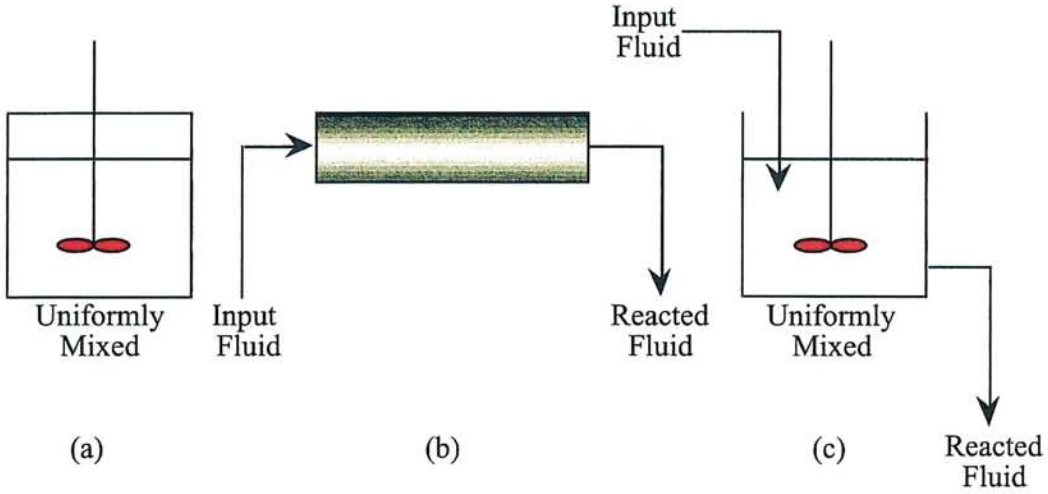

Figure 5 Schematic of column set up

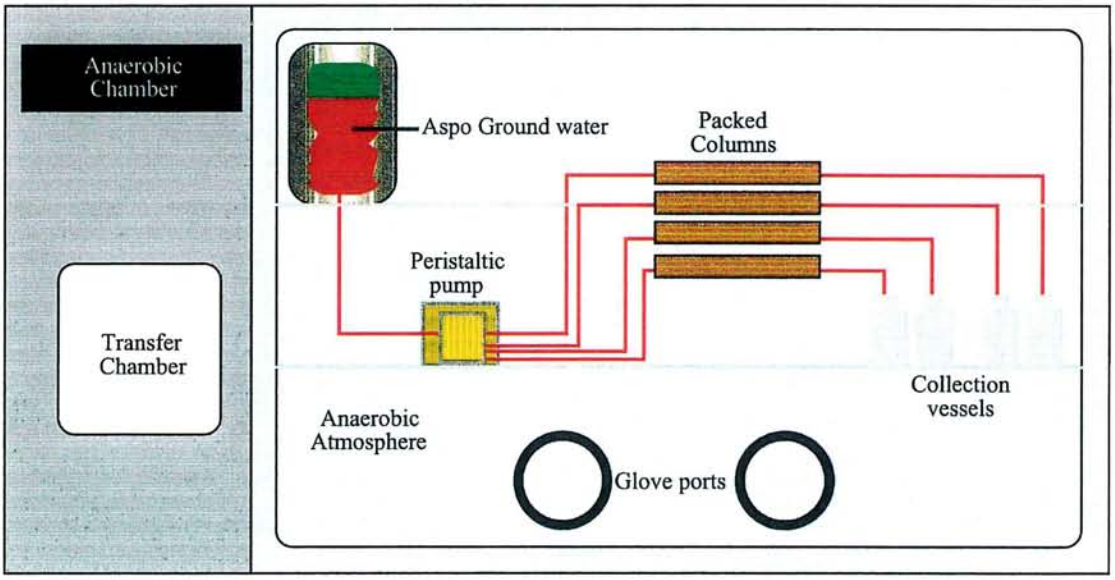

Figure 6 Schematic of CSTR set up

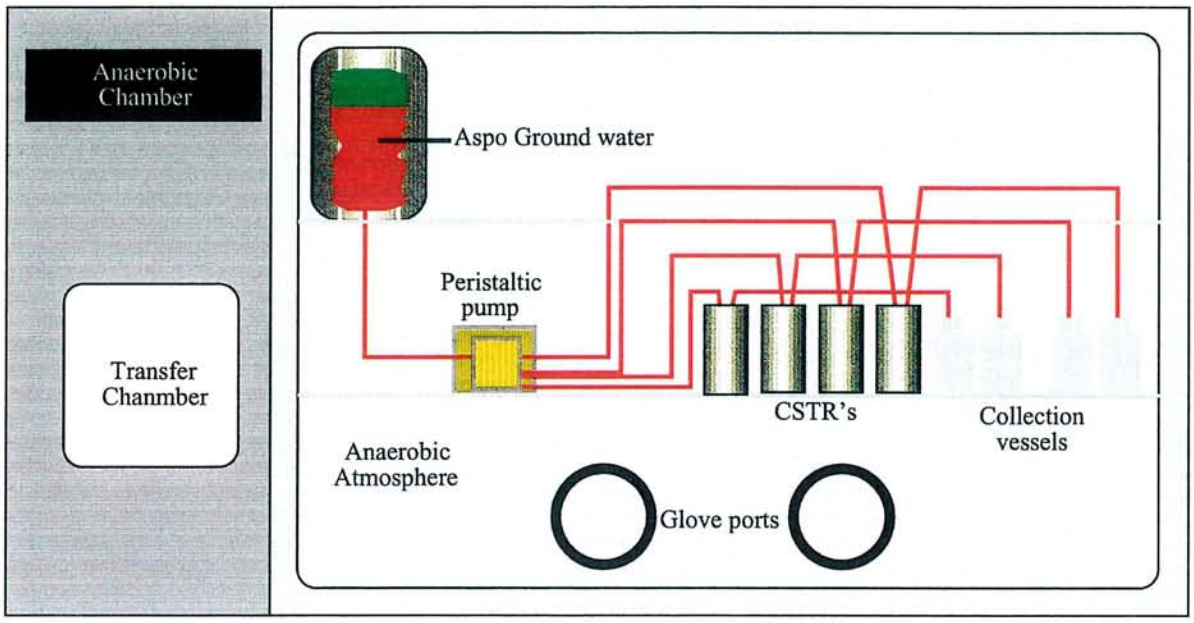

Figure 7 Schematic of CSTR set up

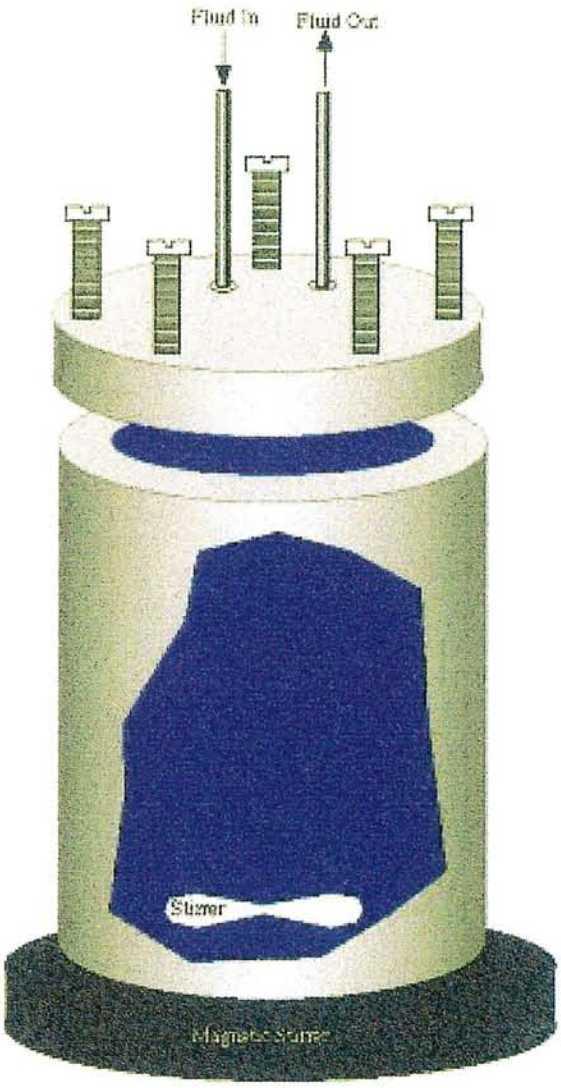

Figure 8 Comparison of the XRD traces (air-dried) obtained from the orientated fine fraction (<5 μm) material separated from the crushed Äspö Diorite starting material and the experimental residue from Column 2.

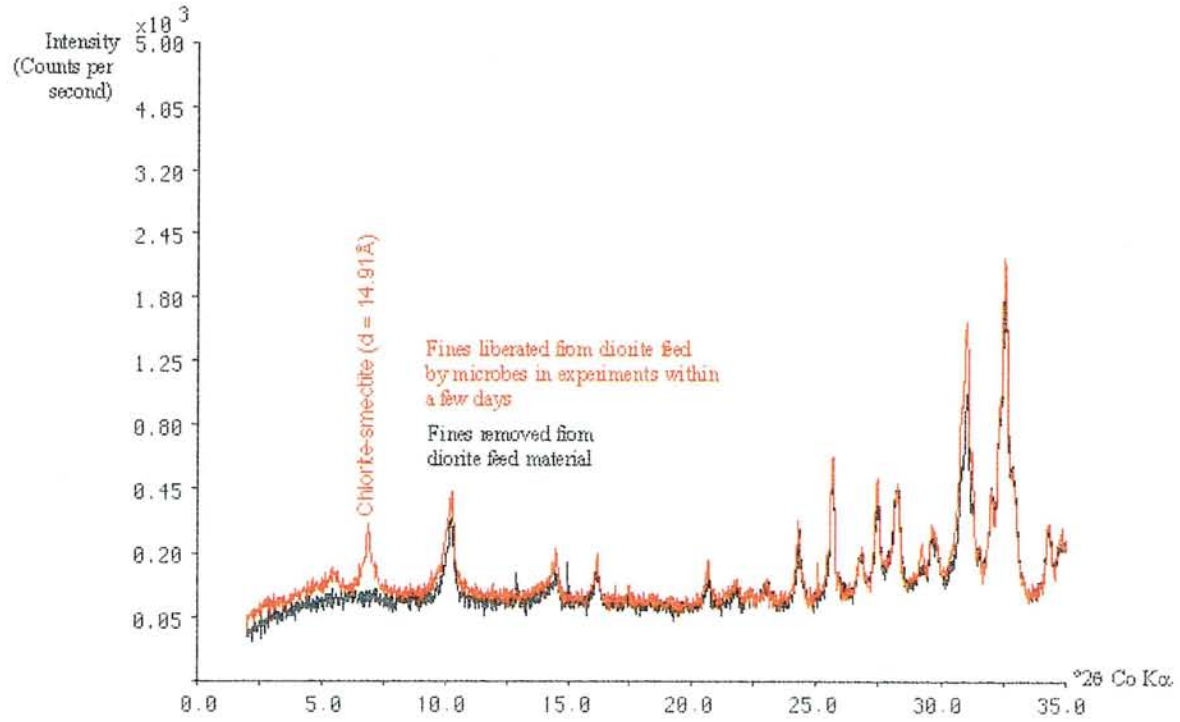

Figure 9 XRD traces (air-dried) obtained from orientated fine fraction (<5 μm) material from CSTR experimental residues: (a) comparison of residues from aerobic experiments with and without bacteria; (b) comparison of residues from anaerobic experiments with and without bacteria.

a)

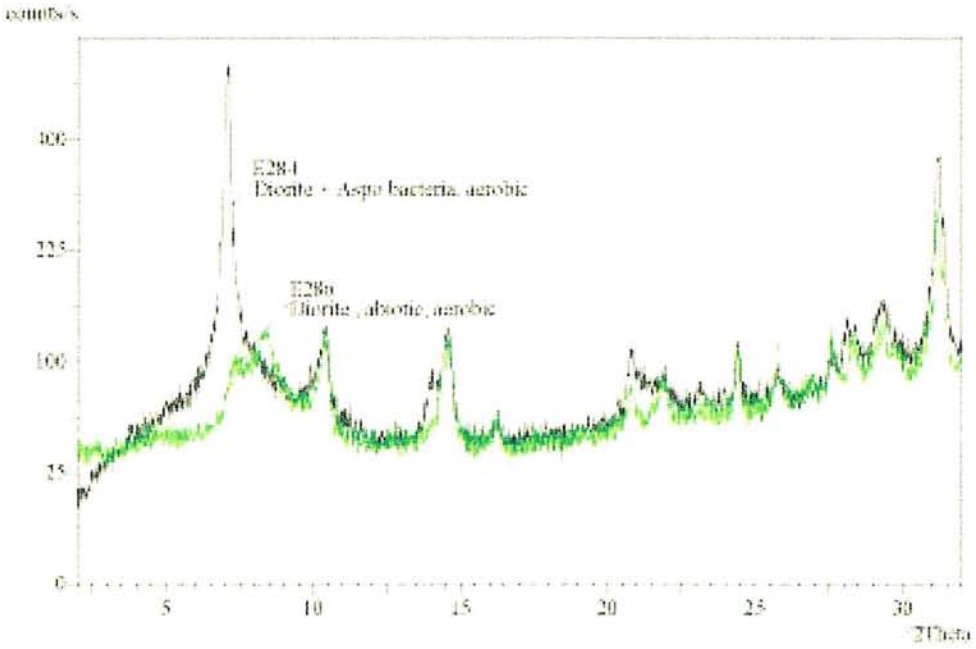

b)

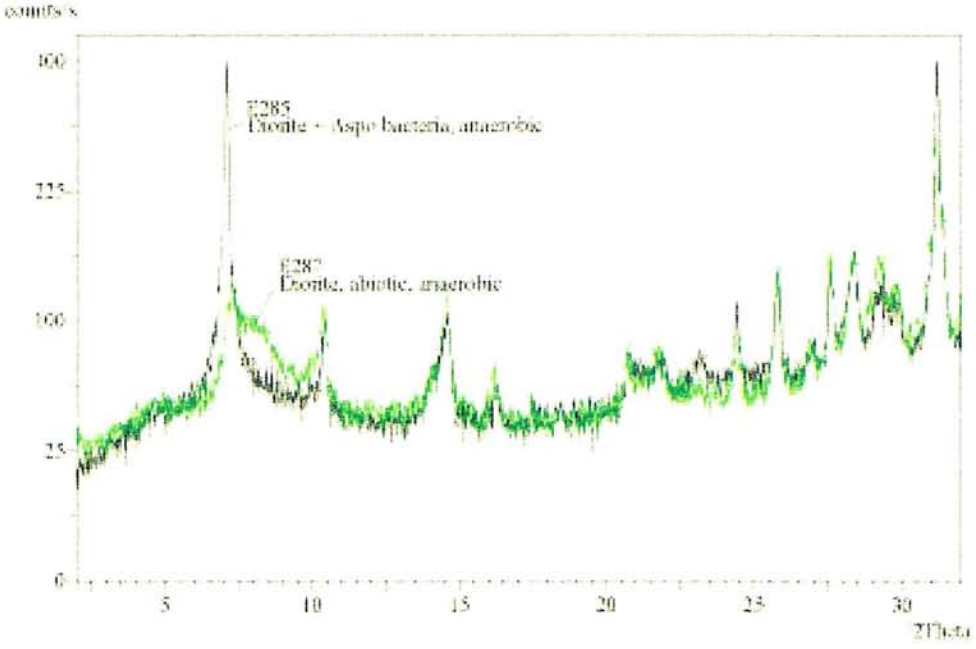

Figure 10 XRD traces (air-dried) obtained from orientated fine fraction (<5 μm) material from CSTR experimental residues: (a) comparison of residues from biotic experiments run under aerobic and anaerobic conditions; (b) comparison of residues from abiotic experiments run under aerobic and anaerobic conditions.

a)

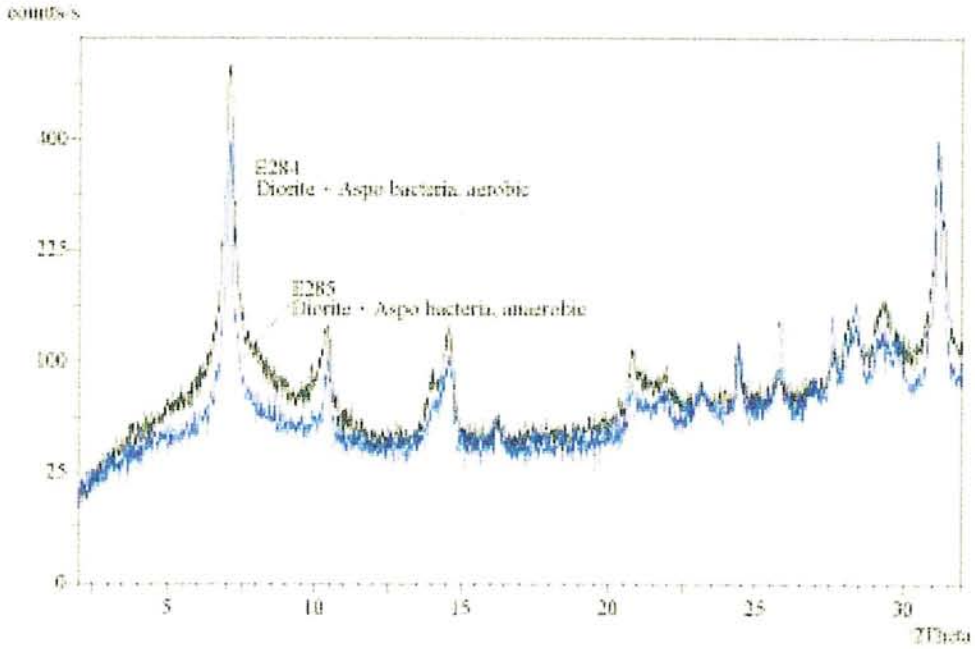

b)

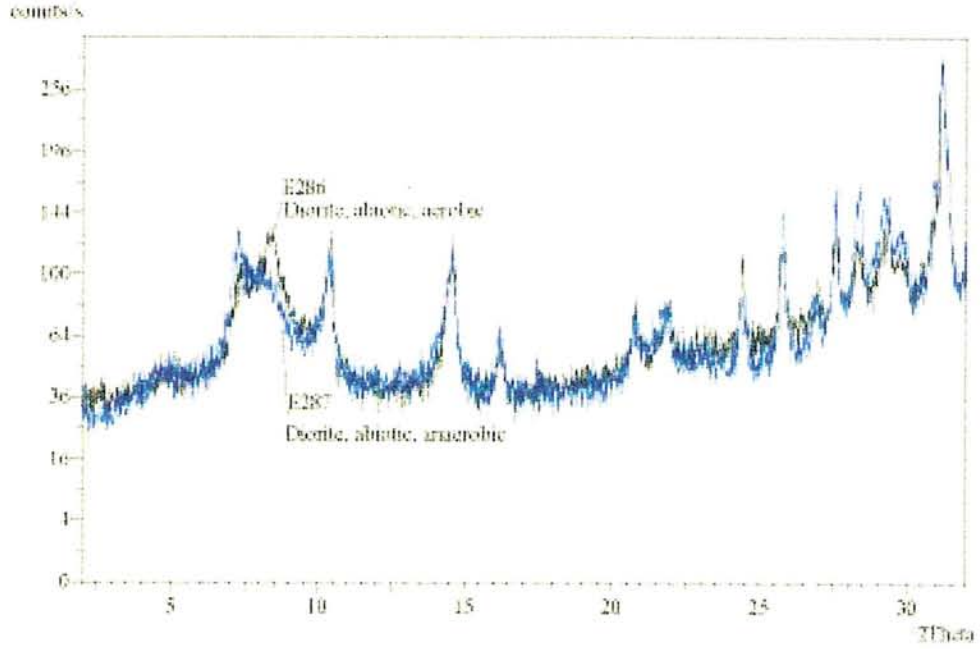

Figure 11 Bacterial Numbers present in vessels

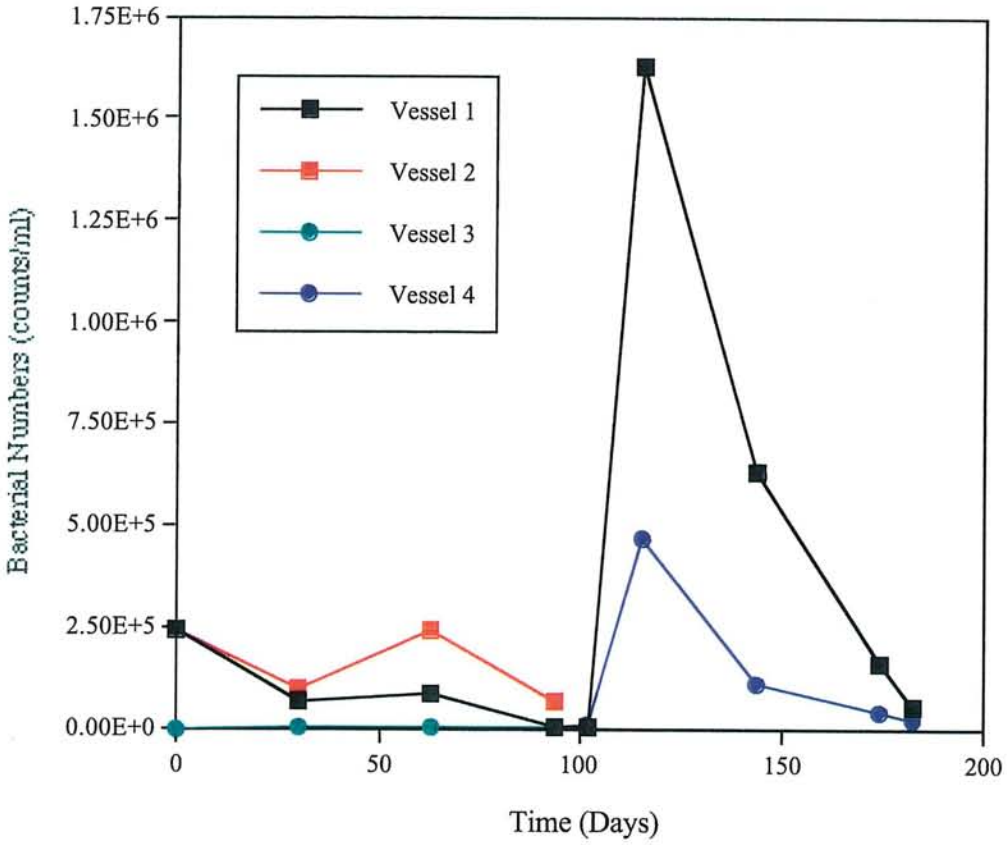

Tables

Table 1 Chemical composition of groundwater samples collected from Äspö borehole KA2858A (September 1997).

Species	Start of collection	End of collection
Field Analyses		
Temp (°C)	14.1	14.2
Eh (mV)	210.0	246.7
pH	8.04	8.25
HCO3 (mg/l)	16	12
Conductivity (μS/cm)	24400	29200
Dissolved O2 (mg/l)	<1	<1
Laboratory Analyses		
pH	6.74	7.16
Ca (mg/l)	3670	4350
Mg (mg/l)	49.7	50.1
Na (mg/l)	2680	2920
K (mg/l)	11.0	12.2
HCO3 (mg/l)	<20	<20
Cl (mg/l)	10309	12405
SO4 (mg/l)	612	664
NO3 (mg/l)	<5.00	<5.00
cation total (meq/l)	305.75	350.82
anion total (meq/l)	304.61	365.03
ionic balance (%)	0.19	-1.99
Br (mg/l)	77.4	94.3
NO2 (mg/l)	<1	<1
HPO4 (mg/l)	0.09	0.12
Total P (mg/l)	<0.10	<0.10
F (mg/l)	1.32	1.29
Total organic carbon (mg/l)	<1.00	1.03
Total inorganic carbon (mg/l)	1.21	1.09
Total S (mg/l)	212	227
Reduced S (μg/l)	13.5	<3.00
NH4 (mg/l)	<0.05	<0.05
Si (mg/l)	4.00	3.81
Ba (mg/l)	0.072	0.088
Sr (mg/l)	56.1	79.9
Mn (mg/l)	0.354	0.369
Total Fe (mg/l)	0.07	0.07
Reduced Fe (mg/l)	0.13	0.14
Al (mg/l)	0.29	0.25
Co (mg/l)	<0.02	<0.02
Ni (mg/l)	<0.02	<0.02
Cu (mg/l)	<0.005	<0.005
Zn (mg/l)	<0.005	<0.005
Cr (mg/l)	<0.01	<0.01
Mo (mg/l)	0.05	0.06
Cd (mg/l)	<0.005	<0.005
Pb (mg/l)	<0.10	<0.10
V (mg/l)	<0.01	<0.01
Li (mg/l)	2.36	2.96
B (mg/l)	1.19	1.10

Table 2 Summary of differences between size fractions of the diorite starting material (MPG sample D337) in terms of peak intensities above background (counts/second).

Peak (°2Q)	Mineral phase	Bulk Diorite	Sand fraction	Fines
10.22	Mica	407	214	551
14.50	Chlorite	93	138	94
31.06	Quartz	1768	1723	1891
32.61	Albite	1611	2384	1463
34.39	Calcite	138	73	142

Table 3 Chemical analysis of diorites

Oxide (wt.%)	C853	D337	D337 Sand fraction	element (ppm)	C853	D337	D337 Sand fraction
SiO_2	59.7	60.20	63.40	Sc	10	9	7
TiO_2	0.77	0.78	0.69	V	69	70	52
Al_2O_3	17.6	17.18	18.21	Cr	26	34	15
$Fe_2O_3^t$		4.95	2.92	Co	14	15	9
$Fe_2O_3^*$	2.27	nd	nd	Ni	17	17	9
FeO^*	2.71	nd	nd	Cu	15	8	14
Mn_3O_4	0.11	0.10	0.07	Zn	86	85	129
MgO	2.01	2.02	0.96	As	<1	<2	<2
CaO	3.81	4.15	3.65	Se	<1	<2	<2
Na_2O	4.35	4.95	6.07	Rb	169	124	89
K_2O	3.76	2.89	2.30	Sr	934	897	964
P_2O_5	0.3	0.32	0.11	Y	20	19	20
SrO	nd	0.12	0.13	Zr	253	273	81
BaO	nd	0.13	0.12	Nb	15	15	15
LOI	1.54	2.14	1.57	Pb	18	22	22
				Ba	1786	1081	1024
Total	99	99.97	100.21				

^{t} = total Fe

* = determined by wet chemical methods

Table 4 Growth media for bacterial cultures

Postgate B medium		Postgate C medium	
KH_2PO_4	0.5 g	KH_2PO_4	0.5 g
NH_4Cl	1.0 g	NH_4Cl	1.0 g
$CaSO_4$	1.0 g	Na_2SO_4	4.5 g
		$CaCl_2.2H_2O$	0.04 g
$MgSO_4.7H_2O$	2.0 g	$MgSO_4.7H_2O$	0.06 g
Sodium lactate	3.5 g	Sodium lactate	6 g
Yeast Extract	1.0 g	Yeast Extract	1.0 g
Ascorbic Acid	0.1 g		
Thioglycollic acid	0.1 g	Sodium citrate	0.3 g
$FeSO_4.7H_2O$	0.5 g	$FeSO_4.7H_2O$	0.004 g
NaCl	7.0 g	NaCl	7.0 g
pH adjusted to between 7.0 and 7.5		pH adjusted to 7.5 ± 0.2 with 1 M NaOH	

IRB medium	
Peptone	0.01 g
$NaHCO_3$	2.5 g
NH_4Cl	1.5 g
NaH_2PO_4	0.6 g
NaCl	0.1 g
$MgCl_2.6H_2O$	0.1 g
$MnCl_2.4H_2O$	0.005 g
$Na_2MoO_4.2H_2O$	0.001 g
Sodium lactate	6.897 g
Yeast Extract	1.0 g
Ascorbic Acid	0.1 g
Thioglycollic acid	0.1 g
Iron Citrate	1.195 g
pH adjusted to 7.0 with 1M HCl	

Table 5 Summary of experiments conducted

Experiment c	Bacteria	Experimental conditions	Comments
Column 1	IRB +SRB	Anaerobic atmosphere	Blocked after 2 weeks reaction
Column 2	IRB + SRB	Anaerobic atmosphere	Blocked after 2 weeks reaction
Column 3	IRB + SRB	Anaerobic atmosphere	Blocked after 2 weeks reaction
Column 4	IRB + SRB	Anaerobic atmosphere	Blocked after 2 weeks reaction
Column 5	none	Anaerobic atmosphere	Terminated after 2 weeks reaction
Column 6	none	Anaerobic atmosphere	Terminated after 2 weeks reaction
Column 7	none	Anaerobic atmosphere	Terminated after 2 weeks reaction
Column 8	none	Anaerobic atmosphere	Terminated after 2 weeks reaction
CSTR 1	IRB + SRB	3 months Anaerobic followed 3 months Aerobic atmosphere	Terminated after 6 months reaction
CSTR 2	IRB + SRB	Anaerobic atmosphere	Terminated after 3 months reaction
CSTR 3	none	Anaerobic atmosphere	Terminated after 3 months reaction
CSTR 4	none	3 months Anaerobic followed 3 months Aerobic atmosphere	Terminated after 6 months reaction

Table 6 Summary of mineralogical techniques used

Experiment	MPG Sample No.	Sample description	Analytical technique
	D337	Diorite starting material	Conventional SEM
Column 2	D761	Column reaction residue – IRB + SRB bacteria added	CryoSEM, Clay XRD
Column 6	D762	Column reaction residue – no added bacteria	CryoSEM, Clay XRD
CSTR 1	E284	Anaerobic reaction residue – IRB + SRB bacteria added	Conventional SEM, Clay XRD
CSTR 2	E285	Anaerobic/Aerobic reaction residue – IRB + SRB bacteria added	Conventional SEM, Clay XRD
CSTR 3	E286	Aerobic reaction residue – no added bacteria	Conventional SEM, Clay XRD
CSTR 4	E287	Anaerobic/Aerobic reaction residue – no added bacteria	Conventional SEM, Clay XRD

Table 7 Bacterial Numbers in vessels (per ml of fluid)

Day	**Vessel 1**	Std error	**Vessel 2**	Std error	**Vessel 3**	Std error	**Vessel 4**	Std error
0	243000	±8400	243000	±8400	0	0	0	0
30	68700	±373	98700	±461	10	0	10	0
63	83100	±1020	240000	±2600	50	0	50	0
94	4990	±236	65700	±632	50	0	50	0
102	2860	±150	-		-		7620	±232
115	1630000	±2820	-		-		468000	±6523
144	628000	±8560	-		-		109000	±3530
174	157000	±8400	-		-		39300	±2510
182	54900	±2740	-		-		23600	±1260

Note: At 100 days, experiments in vessels 2 and 3 were terminated and vessels 1 and 4 were transferred to aerobic atmosphere.

Table 8 Results of chemical Analysis - columns experiments

Sample	Microbes	pH	Ca	Mg	Na	K	Total Alkalinity	Cl	SO_4	NO_3	Br	NO_2
			mg/l	mg/l	mg/l	mg/l	mg/l	mg/l	mg/l	mg/l	mg/l	mg/l
Starting fluid	-	7.16	4350	50.1	2920	12.2	<20	12405	664	<5.00	94.3	<1.00
Column 1, Sample 1	Yes	6.51	4585	68.5	3200	26.1	112	11353	672	<5.00	88.7	<1.00
Column 2 Sample 1	Yes	6.53	4430	65.5	3145	28.6	115	11369	669	<5.00	92.5	<1.00
Column 3 Sample 1	Yes	7.44	4681	69.0	3176	25.3	128	11585	682	<5.00	91.8	<1.00
Column 4 Sample 1	Yes	6.80	4451	66.0	3094	26.9	118	11308	663	<5.00	89.5	<1.00
Column 4 Sample 2	Yes	6.88	4598	66.5	3188	17.4	108	11148	643	<5.00	88.3	<1.00
Column 5 Sample 1	No	7.04	4707	68.0	3196	29.9	185	11633	656	<5.00	92.1	<1.00
Column 5 Sample 1	No	6.91	4537	66.0	3121	29.3	209	11589	661	<5.00	90.5	<1.00
Column 7 Sample 1	No	6.94	4527	65.5	3096	30.5	181	11267	658	<5.00	90.8	<1.00
Column 8 Sample 1	No	6.86	4300	62.5	2993	22.4	186	11213	662	<5.00	91.4	<1.00
Column 8 Sample 2	No	6.99	4581	65.0	3186	16.1	146	11261	635	<5.00	90.7	<1.00
		HPO_4	S_2O_3	TOC	TIC	Total P	Total S	Reduced S	NH_4	Si	SiO_2	Ba
		mg/l	mg/l	mg/l	mg/l	mg/l	mg/l	mg/l	mg/l	mg/l	mg/l	mg/l
Starting fluid	-	0.12		1.0	1.1	<0.10	227	<3.000	<0.05	3.81	8.2	0.088
Column 1, Sample 1	Yes	<0.50	<5.00	16.9	17.9	<2.50	265	<5.000	2.58	8.75	18.7	0.445
Column 2 Sample 1	Yes	<0.50	<5.00	14.5	18.8	<2.50	217	6.200	3.14	8.45	18.1	0.415
Column 3 Sample 1	Yes	1.86	<5.00	15.1	21.6	<2.50	277	<5.000	4.83	10.6	22.6	0.465
Column 4 Sample 1	Yes	<0.50	<5.00	<12.0	21.7	<2.50	262	<5.000	2.50	8.30	17.8	0.450
Column 4 Sample 2	Yes	1.83	<5.00	<12.0	13.8	<2.50	266	<5.000	0.72	8.00	17.1	0.355
Column 5 Sample 1	No	0.80	<5.00	<12.0	25.6	<2.50	242	<5.000	1.44	7.05	15.1	0.530
Column 5 Sample 1	No	<0.50	<5.00	14.7	27.5	<2.50	265	<5.000	1.95	7.65	16.4	0.490
Column 7 Sample 1	No	<0.50	<5.00	<12.0	28.0	<2.50	267	<5.000	1.40	7.55	16.2	0.505
Column 8 Sample 1	No	1.12	<5.00	<12.0	19.9	<2.50	257	<5.000	1.34	7.15	15.3	0.445
Column 8 Sample 2	No	<0.50	<5.00	<12.0	12.3	<2.50	578	<5.000	0.98	7.00	15.0	0.320

Table 9 Results of chemical Analysis - Columns experiments, continued

Sample		Sr	Mn	Total Fe	Reduced Fe	Al	Co	Ni	Cu	Zn	Cr	Mo
		mg/l	mg/l	mg/l	mg/l	mg/l	mg/l	mg/l	mg/l	mg/l	mg/l	mg/l
Starting fluid	-	79.9	0.369	0.1	0.1	0.25	<0.02	<0.02	<0.005	<0.01	0.06	
Column 1, Sample 1	Yes	70.9	1.355	14.0	13.3	2.00	<0.50	<2.50	<0.125	14.3	<0.25	<0.50
Column 2 Sample 1	Yes	71.7	1.405	17.9	16.7	1.65	<0.50	<2.50	<0.125	12.4	<0.25	<0.50
Column 3 Sample 1	Yes	71.8	1.635	22.5	20.9	1.95	<0.50	<2.50	<0.125	14.4	<0.25	<0.50
Column 4 Sample 1	Yes	69.7	1.250	14.0	12.8	2.05	<0.50	<2.50	<0.125	14.9	<0.25	<0.50
Column 4 Sample 2	Yes	72.3	0.875	8.14	7.00	2.15	<0.50	<2.50	<0.125	7.53	<0.25	<0.50
Column 5 Sample 1	No	74.5	1.085	0.48	<0.08	1.60	<0.50	<2.50	<0.125	18.4	<0.25	<0.50
Column 5 Sample 1	No	71.7	1.090	0.81	<0.08	2.15	<0.50	<2.50	<0.125	18.7	<0.25	<0.50
Column 7 Sample 1	No	71.6	1.040	0.57	0.08	2.15	<0.50	<2.50	<0.125	18.6	<0.25	<0.50
Column 8 Sample 1	No	68.9	0.990	0.57	<0.08	1.75	<0.50	<2.50	<0.125	15.5	<0.25	<0.50
Column 8 Sample 2	No	72.9	0.960	2.86	2.30	1.95	<0.50	<2.50	<0.125	1.62	<0.25	<0.50

Sample		Cd	Pb	V	Li	B	Total As	As (III)	As (V)	Total Se	Se (IV)	Se (VI)
		mg/l	mg/l	mg/l	mg/l	mg/l	µg/l	µg/l	µg/l	µg/l	µg/l	µg/l
Starting fluid	-	<0.005	<0.10	<0.01	2.96	1.10						
Column 1, Sample 1	Yes	<0.125	<2.50	<0.25	2.79	1.36	2.29	0.20	2.09	<1.44	<1.36	<1.44
Column 2 Sample 1	Yes	<0.125	<2.50	<0.25	2.68	1.29	1.54	0.17	1.36	<1.44	<1.36	<1.44
Column 3 Sample 1	Yes	<0.125	<2.50	<0.25	2.85	1.41	1.64	0.25	1.39	<1.44	<1.36	<1.44
Column 4 Sample 1	Yes	<0.125	<2.50	<0.25	2.72	1.24	1.51	0.29	1.22	<1.44	<1.36	<1.44
Column 4 Sample 2	Yes	<0.125	<2.50	<0.25	2.77	1.38	1.94	0.41	1.53	<1.44	<1.36	<1.44
Column 5 Sample 1	No	<0.125	<2.50	<0.25	2.80	1.33	1.54	0.22	1.32	<1.44	<1.36	<1.44
Column 5 Sample 1	No	<0.125	<2.50	<0.25	2.76	1.42	1.28	0.18	1.10	<1.44	<1.36	<1.44
Column 7 Sample 1	No	<0.125	<2.50	<0.25	2.69	1.35	1.54	0.34	1.20	<1.44	<1.36	<1.44
Column 8 Sample 1	No	<0.125	<2.50	<0.25	2.61	1.36	1.26	0.08	1.17	<1.44	<1.36	<1.44
Column 8 Sample 2	No	<0.125	<2.50	<0.25	2.76	1.39	1.59	0.46	1.13	<1.44	<1.36	<1.44

Table 10 Results of chemical Analysis - CSTR experiments

Sample	Time (days)	pH	Ca mg/l	Mg mg/l	Na mg/l	K mg/l	Total Alk mg/l	Cl mg/l	SO4 mg/l	NO3 mg/l	Br mg/l	NO2 mg/l	HPO4 mg/l	S2O3 mg/l
Starting fluid	0	7.16	4350	50.1	2920	12.2	<20	12405	664	<5.00	94.3	<1.00	0.12	<5.00
CTSR 1/1	12	7.52	4010	60.4	3180	22.5	119	12116	660	<2.50	95.3	<1.00	0.26	<5.00
CTSR 1/2	22	7.47	3950	57.4	2900	22.4	142	12161	700	<2.50	94.1	<1.00	0.25	<5.00
CTSR 1/3	36	7.71	5140	55.1	2760	22.5	132	11209	646	<2.50	89.4	<1.00	0.25	<5.00
CTSR 1/4	46	7.43	4870	61.0	3130	23.9	136	11517	665	<2.50	93.5	<1.00	0.27	<5.00
CTSR 1/5	56	7.60	4740	65.7	3540	25.3	129	11871	678	<2.50	90.9	<1.00	0.32	<5.00
CTSR 1/6	74	7.61	4920	59.7	3160	18.9	134	11998	675	<2.50	94.9	<1.00	0.29	<5.00
CTSR 1/7	85	7.10	4770	56.5	2970	17.9	126	11715	693	<2.50	98.8	<1.00	0.26	<5.00
CTSR 1/8	106	7.34	5690	64.9	3380	21.6	127	12236	715	<2.50	93.6	<1.00	0.28	<5.00
CTSR 1/9	124	7.51	4450	56.3	3240	36.7	67	11700	673	<2.00	94.2	<0.50	<40.0	<5.00
CTSR 1/10	154	7.15	4440	56.4	3200	31.0	<44	11900	672	<2.00	94.3	<0.50	<40.0	<5.00
CTSR 1/11	183	7.44	4090	55.6	3200	30.0	<44	11800	682	<2.00	95.0	<0.50	<40.0	<5.00
CTSR 2/1	12	7.12	4630	50.1	2510	23.5	119	12182	658	<2.50	91.7	<1.00	0.25	<5.00
CTSR 2/2	22	7.53	4010	56.0	2960	26.7	120	11124	657	<2.50	97.4	<1.00	0.27	<5.00
CTSR 2/3	36	7.57	4660	62.4	3210	26.8	129	11626	662	<2.50	89.8	<1.00	0.30	<5.00
CTSR 2/4	46	7.63	4820	63.7	3350	24.1	143	11977	695	<2.50	96.9	<1.00	0.27	<5.00
CTSR 2/5	56	7.48	4580	53.3	2910	19.6	136	11783	645	<2.50	87.9	<1.00	0.27	<5.00
CTSR 2/6	74	7.42	4740	59.2	3150	22.3	142	11846	691	<2.50	94.7	<1.00	0.29	<5.00
CTSR 3/1	12	7.57	4860	59.8	3100	27.9	139	11536	647	<2.50	89.1	<1.00	0.25	<5.00
CTSR 3/2	22	7.50	4470	55.2	2820	24.9	136	11834	671	<2.50	89.0	<1.00	0.26	<5.00
CTSR 3/3	36	7.48	4830	63.2	3390	28.2	141	11480	691	<2.50	94.9	<1.00	0.28	<5.00
CTSR 3/4	46	7.89	4860	63.7	3370	26.2	150	11618	675	<2.50	97.0	<1.00	0.26	<5.00
CTSR 3/5	56	7.56	4510	65.4	3230	24.2	139	12174	699	<2.50	95.8	<1.00	0.28	<5.00
CTSR 3/6	74	7.41	4390	66.0	3310	26.4	152	12739	711	<2.50	98.6	<1.00	0.31	<5.00
CTSR 4/1	6	7.76	4940	56.3	2860	24.8	155	11437	698	<2.50	99.1	<1.00	0.28	<5.00
CTSR 4/2	14	7.40	4920	56.6	2890	26.9	160	11684	697	<2.50	93.1	<1.00	0.28	<5.00
CTSR 4/3	22	7.49	4440	63.4	3270	29.1	139	11667	638	<2.50	91.5	<1.00	0.26	<5.00
CTSR 4/4	36	7.84	4730	71.5	3080	21.2	108	12128	675	<2.50	91.0	<1.00	0.26	<5.00
CTSR 4/5	56	7.24	4911	65.4	3290	18.3	115	12715	750	<2.50	100.9	<1.00	0.29	<5.00
CTSR 4/6	74	7.59	4320	54.9	3170	36.7	77	11300	655	<2.00	91.5	<0.50	<40.0	<5.00
CTSR 4/7	85	7.54	4390	55.0	3200	33.8	<44	11500	665	<2.00	92.7	<0.50	<40.0	<5.00
CTSR 4/8	97	7.18	4370	55.2	3230	31.8	<44	11900	684	<2.00	94.4	<0.50	<40.0	<5.00
CTSR 4/9	106	7.05	4400	54.7	3220	29.7	<44	11400	671	<2.00	93.9	<0.50	<40.0	<5.00
CTSR 4/10	115	7.08	4410	55.3	3250	29.0	<44	11500	676	<2.00	95.5	<0.50	<40.0	<5.00
CTSR 4/11	134	7.09	4350	54.5	3200	29.2	<44	12200	681	<2.00	95.6	<0.50	<40.0	<5.00

Table 11 Results of chemical Analysis - CSTR experiments, continued

Sample	Time (days)	P mg/l	TOC mg/l	TIC mg/l	Total P mg/l	Total S mg/l	Reduced S µg/l	NH4 mg/l	Si mg/l	SiO2 mg/l	Ba mg/l	Sr mg/l	Mn mg/l
Starting fluid	0	1.29	1.0	1.1	<0.10	227	<3.0	<0.05	3.81	8.2	0.09	79.9	0.369
CTSR 1/1	12	<2.00	31.2	12.8	<0.10	238	<10.0	5.18	6.61	14.1	0.30	75.2	0.788
CTSR 1/2	22	<2.00	19.6	24.5	<0.10	219	<10.0	3.44	6.64	14.2	0.31	68.2	0.724
CTSR 1/3	36	<2.00	10.5	24.0	<0.10	219	10.2	2.15	7.45	15.9	0.29	65.4	0.768
CTSR 1/4	46	<2.00	7.4	29.2	<0.10	244	11.2	3.33	8.11	17.3	0.28	73.3	0.826
CTSR 1/5	56	<2.00	6.7	20.7	<0.10	281	14.9	1.53	8.89	19.0	0.29	83.8	0.909
CTSR 1/6	74	<2.00	6.1	24.0	<0.10	259	<10.0	2.29	6.98	14.9	0.23	75.6	0.840
CTSR 1/7	85	<2.00	5.4	25.1	<0.10	237	17.1	1.34	6.47	13.8	0.22	73.2	0.837
CTSR 1/8	106	<2.00	5.1	23.3	0.13	254	<10.0	4.45	7.22	15.4	0.25	80.2	0.905
CTSR 1/9	124	<2.50	<6.00	<3.00	0.14	228	<5.0	<1.95	6.68	14.3	0.19	53.8	0.599
CTSR 1/10	154	<2.50	<6.00	5.2	0.16	228	<5.0	<1.95	6.39	13.7	0.23	54.2	0.523
CTSR 1/11	183	<2.50	<6.00	23.4	0.18	229	<5.0	<1.95	5.18	11.1	0.56	53.6	0.382
					0.17	215	<5.0	<1.95	4.71	10.1	0.73	53.6	0.390
CTSR 2/1	12	<2.00	48.0	22.5	<0.10	203	19.8	2.01	5.34	11.4	0.32	60.0	0.649
CTSR 2/2	22	<2.00	25.6	19.0	<0.10	229	175.2	2.53	6.29	13.5	0.33	68.8	0.726
CTSR 2/3	36	<2.00	16.2	23.3	<0.20	258	26.9	1.52	6.99	15.0	0.31	75.8	0.826
CTSR 2/4	46	<2.00	14.6	18.4	<0.10	255	11.8	4.29	6.93	14.8	0.28	79.2	0.884
CTSR 2/5	56	<2.00	8.9	24.4	<0.10	227	13.9	1.17	6.38	13.6	0.24	67.7	0.791
CTSR 2/6	74	<2.00	8.1	29.9	0.11	247	12.8	4.18	6.81	14.6	0.26	74.9	0.835
CTSR 3/1	12	<2.00	22.3	18.9	<0.10	252	<10.0	1.52	7.53	16.1	0.38	76.9	0.837
CTSR 3/2	22	<2.00	12.5	26.9	<0.20	219	14.0	2.50	6.86	14.7	0.31	67.1	0.745
CTSR 3/3	36	<2.00	10.7	26.6	<0.10	255	48.4	2.58	8.22	17.6	0.35	79.7	0.836
CTSR 3/4	46	<2.00	7.5	31.7	<0.10	266	<10.0	1.89	8.69	18.6	0.31	80.1	0.879
CTSR 3/5	56	<2.00	6.1	24.6	<0.20	259	<10.0	1.43	9.64	20.6	0.32	75.8	0.855
CTSR 3/6	74	<2.00	8.0	29.9	<0.10	267	<10.0	4.65	10.80	23.1	0.35	82.0	0.993
CTSR 4/1	6	<2.00	28.6	34.2	<0.10	226	11.3	0.90	6.81	14.6	0.33	66.4	0.761
CTSR 4/2	14	<2.00	43.6	19.7	<0.10	244	21.9	2.26	6.91	14.8	0.38	67.7	0.815
CTSR 4/3	22	<2.00	22.0	16.8	<0.10	260	21.9	0.59	8.91	19.1	0.39	77.3	0.900
CTSR 4/4	36	<2.00	8.6	27.1	<0.10	277	<10.0	1.30	8.24	17.6	0.28	87.8	0.695
CTSR 4/5	56	<2.00	5.7	27.2	<0.10	261	11.8	5.86	7.23	15.5	0.23	79.3	0.759
CTSR 4/6	74	<2.50	<6.00	5.7	0.17	227	<5.0	<1.95	6.83	14.6	0.40	53.2	0.534
CTSR 4/7	85	<2.50	<6.00	31.8	0.17	237	<5.0	<1.95	5.79	12.4	0.21	53.6	0.394
CTSR 4/8	97	<2.50	<6.00	4.2	0.50	232	<5.0	<1.95	4.55	9.7	0.24	54.1	0.255
CTSR 4/9	106	<2.50	<6.00	13.7	0.19	232	<5.0	<1.95	5.25	11.2	0.22	53.9	0.331
CTSR 4/10	115	<2.50	<6.00	<3.00	0.16	232	<5.0	<1.95	4.98	10.7	0.27	54.1	0.300
CTSR 4/11	134	<2.50	<6.00	3.6	0.17	227	<5.0	<1.95	5.16	11.0	0.31	53.7	0.323

Table 12 Results of chemical Analysis - CSTR experiments, continued

Sample	Time (days)	Total Fe mg/l	Reduced Fe mg/l	Al mg/l	Co mg/l	Ni mg/l	Cu mg/l	Zn mg/l	Cr mg/l	Mo mg/l	Cd mg/l	Pb mg/l
Starting fluid	0	0.07	0.14	0.25	<0.020	<0.020	<0.005	<0.01	<0.01	0.060	<0.0005	<0.10
CTSR 1/1	12	0.35	1.65	1.69	<0.020	0.072	0.060	3.21	<0.01	0.065	<0.0005	<0.10
CTSR 1/2	22	0.04	0.45	1.69	<0.020	0.064	0.043	1.86	<0.01	<0.020	<0.0005	<0.10
CTSR 1/3	36	0.13	0.29	2.47	<0.020	0.062	0.031	0.98	<0.01	0.063	<0.0005	<0.10
CTSR 1/4	46	0.08	0.16	1.74	<0.020	0.059	0.010	0.62	<0.01	0.067	<0.0005	<0.10
CTSR 1/5	56	<0.05	<0.09	1.76	<0.020	0.055	<0.005	0.52	<0.01	0.058	<0.0005	<0.10
CTSR 1/6	74	<0.05	<0.09	1.75	<0.020	0.081	<0.005	0.40	<0.01	0.053	<0.0005	<0.10
CTSR 1/7	85	<0.05	<0.09	1.52	<0.020	0.060	<0.005	0.32	<0.01	0.067	<0.0005	<0.10
CTSR 1/8	106	<0.05	0.23	1.80	<0.020	0.053	<0.005	0.29	<0.01	0.047	<0.0005	<0.10
CTSR 1/9	124	<0.01	<0.09	0.09	<0.005	0.041	<0.010	0.22	<0.01	0.048	<0.0000	<0.05
CTSR 1/10	154	<0.01	<0.09	0.03	<0.005	<0.020	<0.010	0.06	<0.01	0.055	<0.0000	<0.05
CTSR 1/11	183	<0.01	<0.09	0.02	<0.005	<0.020	<0.010	0.02	<0.01	0.049	<0.0000	<0.05
		<0.01	<0.09	0.03	0.120	0.069	<0.010	0.02	<0.01	0.055	0.001	<0.05
CTSR 2/1	12	0.03	0.32	1.31	<0.020	0.085	0.091	5.56	<0.01	0.070	<0.0005	<0.10
CTSR 2/2	22	0.09	<0.09	1.59	<0.020	0.075	0.044	2.72	<0.01	0.069	<0.0005	<0.10
CTSR 2/3	36	0.03	0.39	1.62	<0.040	0.073	<0.010	1.48	<0.02	0.056	<0.0005	<0.10
CTSR 2/4	46	0.22	0.29	1.73	<0.020	0.069	<0.005	0.88	<0.01	0.062	<0.0005	<0.10
CTSR 2/5	56	<0.05	<0.09	1.85	<0.020	0.079	<0.005	0.80	<0.01	0.060	<0.0005	<0.10
CTSR 2/6	74	<0.05	<0.09	1.47	<0.020	0.067	<0.005	0.60	<0.01	0.064	<0.0005	<0.10
CTSR 3/1	12	0.22	0.49	1.67	<0.020	0.064	0.111	2.55	<0.01	0.051	<0.0005	<0.10
CTSR 3/2	22	0.06	0.23	1.63	<0.040	0.073	0.070	1.69	<0.02	0.052	<0.0005	<0.10
CTSR 3/3	36	0.22	0.49	1.83	<0.020	0.083	0.030	0.98	<0.01	0.066	<0.0005	<0.10
CTSR 3/4	46	0.20	0.39	1.74	<0.020	0.075	0.020	0.61	<0.01	0.046	<0.0005	<0.10
CTSR 3/5	56	<0.02	0.61	1.69	<0.040	0.086	0.012	0.53	<0.02	0.060	<0.0005	<0.10
CTSR 3/6	74	<0.05	0.32	1.75	<0.020	0.062	<0.005	0.36	<0.01	0.059	<0.0005	<0.10
CTSR 4/1	6	0.18	0.45	1.64	<0.020	0.069	0.050	2.22	<0.01	<0.020	<0.0005	0.15
CTSR 4/2	14	<0.05	<0.09	1.80	<0.020	0.064	<0.005	3.26	<0.01	0.068	<0.0005	<0.10
CTSR 4/3	22	0.03	0.65	1.64	0.037	0.080	<0.005	1.19	<0.01	0.051	<0.0005	<0.10
CTSR 4/4	36	<0.05	0.26	1.77	0.028	0.061	<0.005	0.58	<0.01	0.054	<0.0005	<0.10
CTSR 4/5	56	0.01	0.26	1.73	0.023	0.054	<0.005	0.43	<0.01	0.066	<0.0005	<0.10
CTSR 4/6	74	<0.01	<0.09	0.03	0.037	0.031	0.011	0.11	<0.01	0.053	0.0001	<0.05
CTSR 4/7	85	<0.01	<0.09	0.04	0.021	0.021	<0.010	0.03	<0.01	0.054	<0.0000	<0.05
CTSR 4/8	97	<0.01	<0.09	0.02	0.008	<0.020	0.011	0.02	<0.01	0.038	<0.0000	<0.05
CTSR 4/9	106	<0.01	<0.09	0.03	0.009	<0.020	0.012	0.02	<0.01	0.053	<0.0000	<0.05
CTSR 4/10	115	<0.01	<0.09	0.03	0.009	<0.020	0.013	0.02	<0.01	0.049	<0.0000	<0.05
CTSR 4/11	134	<0.01	<0.09	0.02	0.011	<0.020	<0.010	0.02	<0.01	0.054	<0.0000	<0.05

Table 13 Results of chemical Analysis - CSTR experiments, continued

Sample	Time (days)	V mg/l	Li mg/l	B mg/l	As (T) ug/l	As (III) ug/l	As(V) ug/l	Se (T) ug/l	Se (IV) ug/l	Se (VI) ug/l
Starting fluid	0	<0.01	2.96	1.10	-	-	-	-	-	-
CTSR 1/1	12	<0.01	2.80	1.35	10.4	8.90	1.46	<0.50	<0.50	<0.50
CTSR 1/2	22	<0.01	2.52	1.18	9.2	9.23	<0.01	<0.50	<0.50	<0.50
CTSR 1/3	36	<0.01	2.41	1.16	7.7	8.27	<0.53	<0.50	<0.50	<0.50
CTSR 1/4	46	<0.01	2.58	1.32	8.1	8.80	<0.72	<0.50	<0.50	<0.50
CTSR 1/5	56	<0.01	3.07	1.50	7.6	8.75	<1.12	<0.50	<0.50	<0.50
CTSR 1/6	74	<0.01	2.67	1.31	2.7	4.23	<1.51	<0.50	<0.50	<0.50
CTSR 1/7	85	<0.01	2.68	1.28	3.3	4.04	<0.75	<0.50	<0.50	<0.50
CTSR 1/8	106	<0.01	2.99	1.39	3.4	3.94	<0.54	<0.50	<0.50	<0.50
CTSR 1/9	124	<0.01	2.49	1.61	6.3	6.30	0.04	<1.00	<1.00	<1.00
CTSR 1/10	154	<0.01	2.49	1.53	6.1	5.09	1.00	<1.00	<1.00	<1.00
CTSR 1/11	183	<0.01	2.49	1.56	6.8	5.45	1.38	<1.00	<1.00	<1.00
		<0.01	2.49	1.47	6.6	4.96	1.62	<1.00	<1.00	<1.00
CTSR 2/1	12	<0.01	2.26	1.10	8.8	9.09	<0.33	<0.50	<0.50	<0.50
CTSR 2/2	22	<0.01	2.56	1.25	8.1	8.75	<0.67	<0.50	<0.50	<0.50
CTSR 2/3	36	<0.02	2.70	1.34	9.0	8.51	0.48	<0.50	<0.50	<0.50
CTSR 2/4	46	<0.01	2.90	1.39	7.9	7.93	<0.07	<0.50	<0.50	<0.50
CTSR 2/5	56	<0.01	2.48	1.21	7.3	7.93	<0.64	<0.50	<0.50	<0.50
CTSR 2/6	74	<0.01	2.69	1.28	3.3	4.04	<0.75	<0.50	<0.50	<0.50
CTSR 3/1	12	<0.01	2.74	1.34	8.5	8.80	<0.26	<0.50	<0.50	<0.50
CTSR 3/2	22	<0.02	2.49	1.21	7.3	8.12	<0.84	<0.50	<0.50	<0.50
CTSR 3/3	36	<0.01	2.81	1.35	8.2	9.14	<0.95	<0.50	<0.50	<0.50
CTSR 3/4	46	<0.01	2.85	1.36	9.4	9.09	0.36	<0.50	<0.50	<0.50
CTSR 3/5	56	<0.02	2.65	1.36	7.5	8.22	<0.71	<0.50	<0.50	<0.50
CTSR 3/6	74	<0.01	2.74	1.26	3.2	3.94	<0.77	<0.50	<0.50	<0.50
CTSR 4/1	6	<0.01	2.50	1.25	16.4	11.67	4.75	<0.50	<0.50	<0.50
CTSR 4/2	14	<0.01	2.49	1.24	4.2	4.33	<0.15	<0.50	<0.50	<0.50
CTSR 4/3	22	<0.01	2.88	1.35	7.3	8.60	<1.31	<0.50	<0.50	<0.50
CTSR 4/4	36	<0.01	3.02	1.24	2.0	3.46	<1.47	<0.50	<0.50	<0.50
CTSR 4/5	56	<0.01	2.75	1.31	2.8	3.75	<0.96	<0.50	<0.50	<0.50
CTSR 4/6	74	<0.01	2.49	1.56	8.3	5.93	2.39	<1.00	<1.00	<1.00
CTSR 4/7	85	<0.01	2.49	1.55	8.8	5.69	3.12	<1.00	<1.00	<1.00
CTSR 4/8	97	<0.01	2.50	1.55	8.8	5.33	3.49	<1.00	<1.00	<1.00
CTSR 4/9	106	<0.01	2.50	1.58	7.3	5.81	1.51	<1.00	<1.00	<1.00
CTSR 4/10	115	<0.01	2.51	1.56	6.8	4.72	2.11	<1.00	<1.00	<1.00
CTSR 4/11	134	<0.01	2.49	1.56	6.1	4.96	1.12	<1.00	<1.00	<1.00

Table 14 Results of stable isotope analysis - CSTR experiments

Sample	Time (days)	$\delta^{34}S$ (SO_4) ‰VCDT	Sample	Time (days)	$\delta^{34}S$ (SO_4) ‰VCDT
Starting fluid	0	8.3			
CTSR 1/1	12	9.8	**CTSR 3/1**	12	10.8
CTSR 1/2	22	10.3	**CTSR 3/2**	22	11.1
CTSR 1/3	36	10.9	**CTSR 3/3**	36	11
CTSR 1/4	46	10.7	**CTSR 3/4**	46	11
CTSR 1/5	56	11.2	**CTSR 3/5**	56	10.9
CTSR 1/6	74	11.4	**CTSR 3/6**	74	10.8
CTSR 1/7	85	10			
CTSR 1/8	106	9.5	**CTSR 4/1**	6	10.8
CTSR 1/9	124	9.9	**CTSR 4/2**	14	11
CTSR 1/10	154	10.2	**CTSR 4/3**	22	9.5
CTSR 1/11	183	9.5	**CTSR 4/4**	36	10.7
			CTSR 4/5	56	9.2
CTSR 2/1	12	9.5	**CTSR 4/6**	74	10.8
CTSR 2/2	22	9.9	**CTSR 4/7**	85	10
CTSR 2/3	36	9.5	**CTSR 4/8**	97	10.4
CTSR 2/4	46	11.1	**CTSR 4/9**	106	10.7
CTSR 2/5	56	11	**CTSR 4/10**	115	10.1
CTSR 2/6	74	9.3	**CTSR 4/11**	134	10.4

Note: The results of the stable isotope analysis are expressed as $\delta^{34}S$ as permil (‰) deviation from the VCDT standard with an overall analytical reproducibility of ±0.1‰. Reference materials IAEA-S-1 gave -0.3‰ and NBS122 gave 0.15‰.

Plates

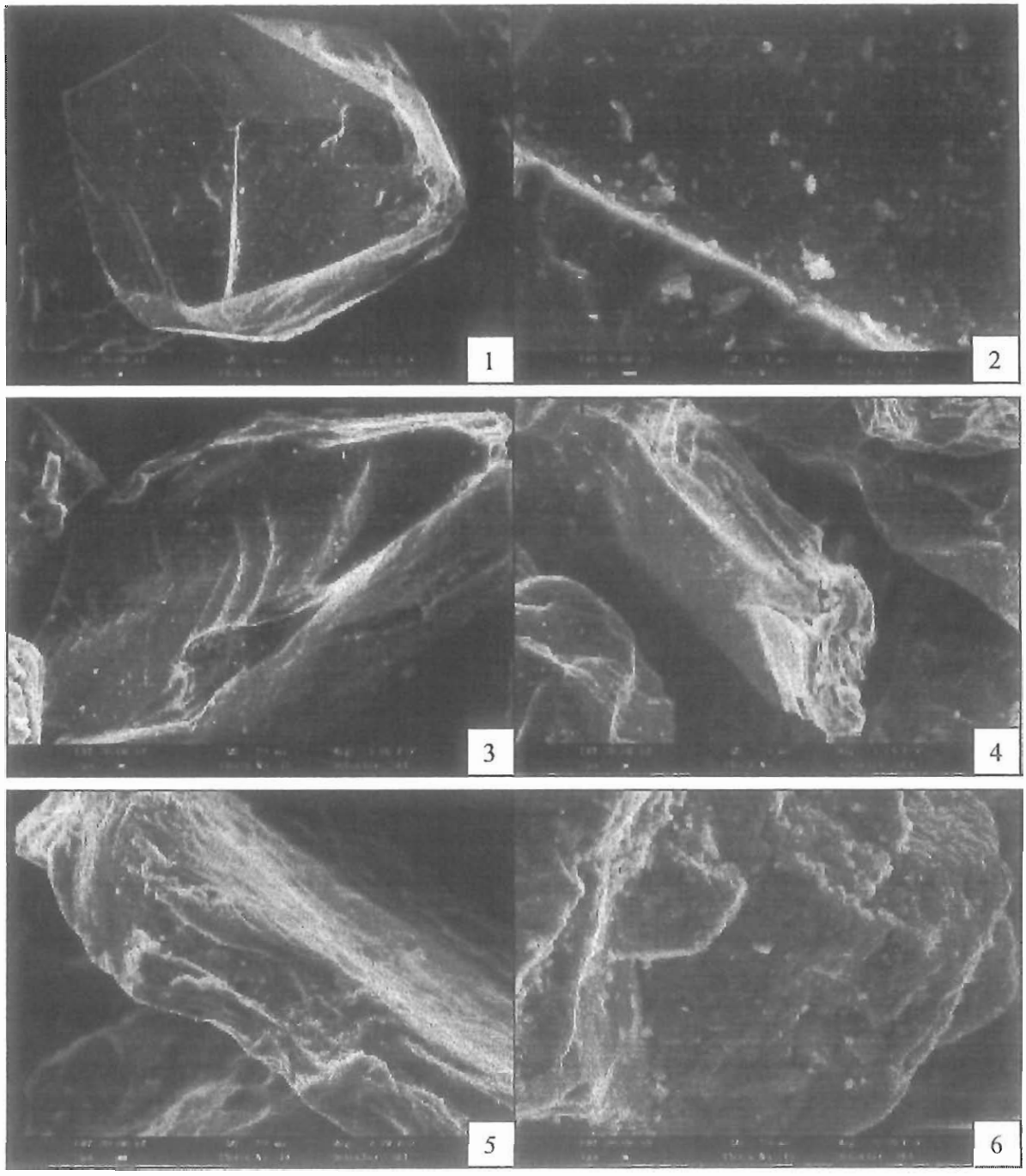

Plate 1 Magnetite showing unaltered grain surfaces coated with fines from the sample preparation process. (D337S102).

Plate 2 Detail of fine grained particles on unaltered magnetite surface showing angular nature of fines derived from crushing processes. (D337S103).

Plate 3 Quartz grain showing subconchoidal fracture surfaces and sharp grain edges. Note fine grained material adhering to grain surface. (D337S108).

Plate 4 Biotite showing evidence of mechanical distortion; folding of grain edges and minor opening along the basal cleavage plane. (D337S105).

Plate 5 Detail of biotite grains showing fine grained particles, generated by crushing, lodged in intra-grain spacing along the basal cleavage plane. (D337S107).

Plate 6 Calcite showing extensive corrosion and dissolution textures. (D337S112)

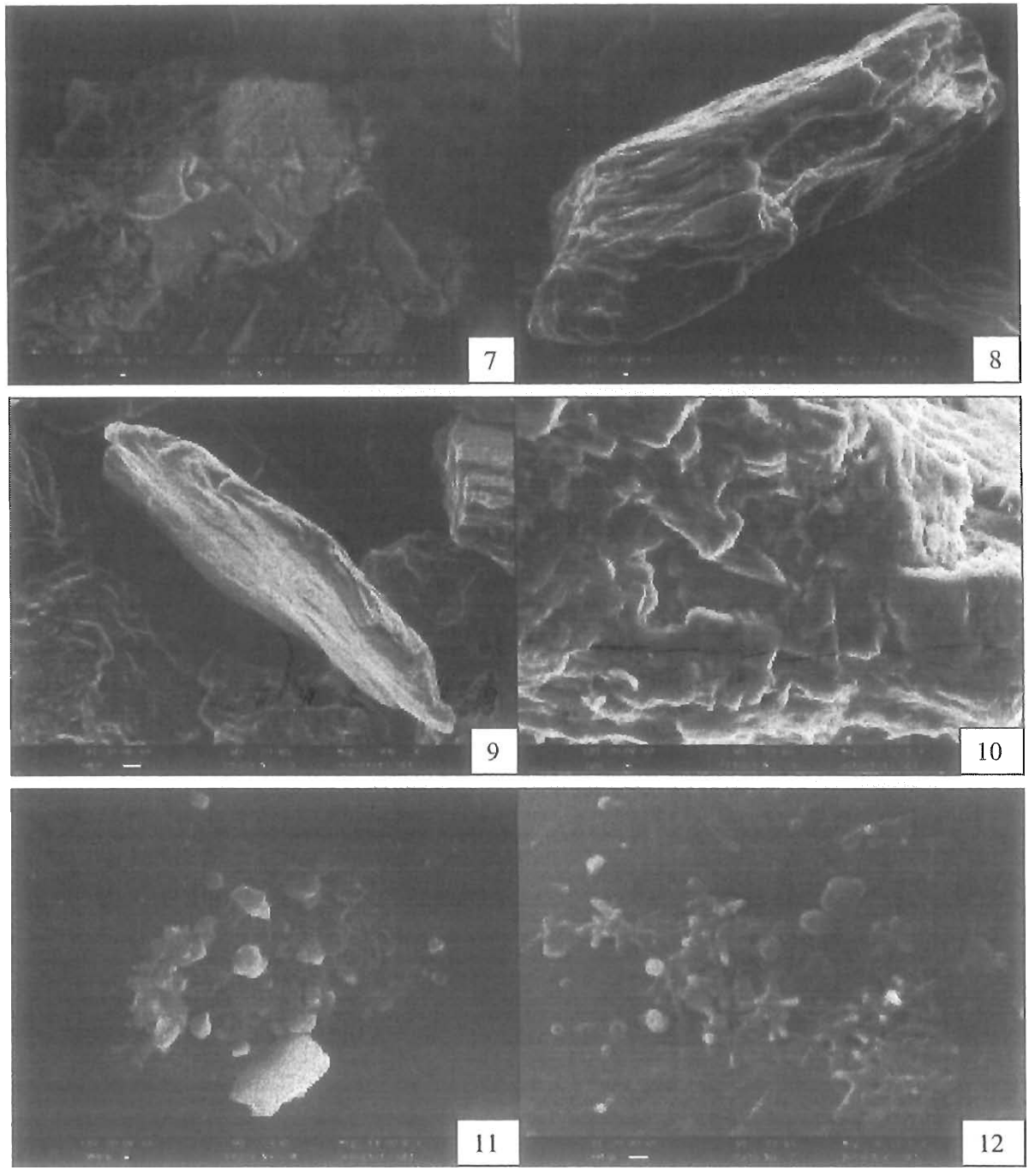

Plate 7 Back scattered electron image of calcite showing near pristine fractured crystal surfaces, in contrast to textures seen in Plate 6. (E337S113)

Plate 8 Biotite grain from CSTR Run 2 showing minor increase in the degree of exfoliation and minor dissolution of plate edges relative to the starting material. (E285S103).

Plate 9 Biotite (CSTR Run 3) showing folding of plate edges due to either initial sample preparation or mechanical attrition in the CSTR environment. Exfoliation is similar to that seen in CSTR Run 2. (E286S101).

Plate 10 Etched calcite surfaces observed from CSTR Run 2. (E285S105).

Plate 11 Fine grained particles present on quartz surface in CSTR 2. (E285S108).

Plate 12 Fine grained material present on quartz grain surface in CSTR Run 1. EDXA indicates clay and gypsum chemistries. (E284S104)

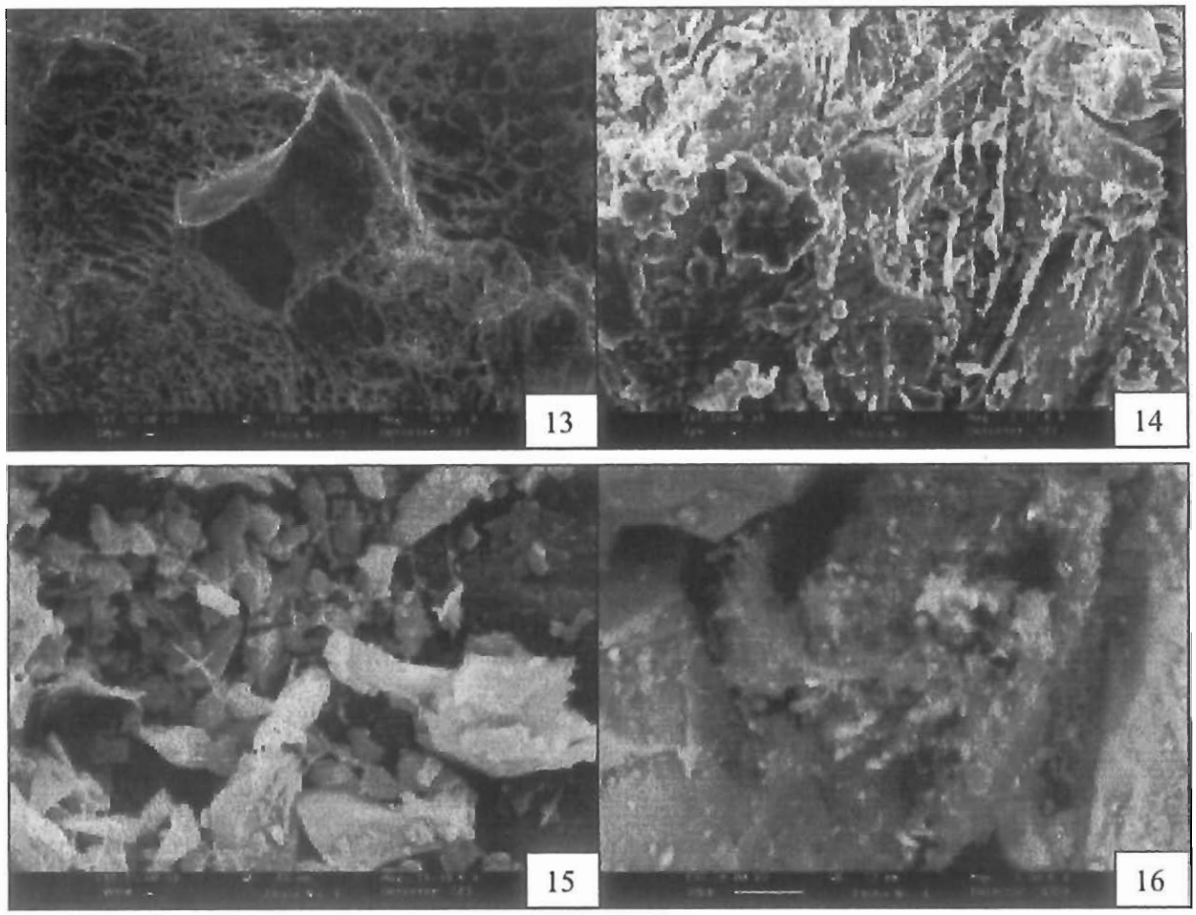

Plate 13 Extensive filamentous meshwork of salt in cryoSEM samples due to precipitation from saline pore water during sublimation of ice glass. Column 6 (D762S202)

Plate 14 Clustering of salt crystals contaminating grain surfaces on samples, after washing with de-ionised water, prior to cryoSEM. Column 2 (D761C102).

Plate 15 Organic filaments entrapping fine-grained diorite material and possible smectitic or chloritic clays formed during experiments. Column 2 (D761C104).

Plate 16 Cryo-SEM photomicrograph showing the formation of minor amounts of smectite clay precipitate on grain surfaces. Column 2. (D761C304).